

Astrophysical implications of high energy neutrino limits

Julia K. Becker ^{a,*} , Andreas Groß ^{a,b} , Kirsten Münich ^a
 Jens Dreyer ^a , Wolfgang Rhode ^a , Peter L. Biermann ^{c,d,e}

^a*Universität Dortmund, Institut für Physik, D-44221 Dortmund, Germany*

^b*Max-Planck-Institut für Kernphysik, D-69177 Heidelberg, Germany*

^c*Max Planck Institut für Radioastronomie, Auf dem Hügel 69, D-53121 Bonn, Germany*

^d*Department of Physics and Astronomy, University of Bonn, Germany*

^e*Department of Physics and Astronomy, University of Alabama, Tuscaloosa, Alabama 35487, USA*

Abstract

Second generation high energy neutrino telescopes are being built to reach sensitivities of neutrino emission from galactic and extragalactic sources. Current neutrino detectors are already able to set limits which are in the range of some emission models. In particular, the **A**ntarctic **M**uon **A**nd **N**eutrino **D**etection **A**rray (AMANDA) has recently presented the so far most restrictive limit on diffuse neutrino emission (Achterberg et al. (IceCube Coll.), 2007). Stacking limits which apply to AGN point source classes rather than to single point sources Achterberg et al. (IceCube Coll. & P. L. Biermann) are given as well. In this paper, the two different types of limits will be used to draw conclusions about different emission models. An interpretation of stacking limits as diffuse limits to the emission from considered point source class is presented. The limits can for instance be used to constrain the predicted correlation of EGRET-detected diffuse emission and neutrino emission. Also, the correlation between X-ray and neutrino emission is constrained. Further results for source classes like TeV blazars and FR-II galaxies are presented. Starting from the source catalogs so-far examined for the stacking method, we discuss further potential catalogs and examine the possibilities of the second generation telescopes ICECUBE and KM3NET by comparing catalogs with respect to northern and southern hemisphere total flux.

Key words: AGN, neutrinos, stacking, diffuse spectra, limits, Olbers paradox

PACS: 95.55.Vj, 95.80.+p, 95.85.Pw, 95.85.Ry

1 Introduction

As is well known for hundreds of years, the sky would be infinitely bright in optical light, if all space were homogeneously full of stars, and space were infinitely extended without any change in properties (Olbers, 1826). This reasoning can be applied to stars as well as to galaxies. This argument can also be applied to electromagnetic emissions and just as well to neutrino emission. The solution to Olbers paradox is that space is not homogeneously full of identical distributions of stars or galaxies, and that the Universe evolves quite strongly. This implies that the integral over the optical light of all galaxies has a finite sum, which does not exceed an observable level. Clearly, given a proper sampling of galaxies, it is possible to determine this level. In some cases, there is a unique relationship between the optical light and the emission at some other wavelength. Starting from this correlation, the summed emission from all galaxies over all history can be deduced and it is a simple function of the sum at optical wavelengths. The optical emission can certainly be replaced with the emission at some other electromagnetic wavelength, such as X-rays. Equally, the correlated wavelength can be neutrino emission. If we now do not know what the sum of the emission is at the electromagnetic wavelength, but have limits, then a limit for the neutrino emission can be deduced a fortiori. Vice versa, if we have a limit for the neutrino emission, a corresponding limit for the electromagnetic emission can be derived. In either case, it might happen, that we have a known background, and then can deduce whether this specific class of sources could possibly explain all background at the other "wavelength". We start this argument with neutrinos, set a limit, and then derive a limit for the electromagnetic background. We could also start with the electromagnetic background, and then set a limit for the neutrino emission. So we have an *Olbers paradox for neutrinos*. This is the key point of this paper.

More concretely, the interpretation of different AMANDA neutrino flux limits is done for different classes of Active Galactic Nuclei (AGN). In the case of a stacking analysis in which the strongest sources from the same class are selected, a method for the interpretation of these limits as limits to the diffuse flux from the given source class is developed. Additionally, future possibilities of second generation neutrino telescopes like ICECUBE and KM3NET are examined. Different source classes are discussed with respect to their distribution in the sky, i.e. which sources are in the northern and which are in the southern hemisphere. The field of view for ICECUBE respectively KM3NET is the northern respectively the southern hemisphere and their view of the sky is complementary.

* Corresponding author. Contact: julia.becker@udo.edu, phone: +49-231-7553667

This paper is organized as follows: in Section 2, the prevailing models are discussed according to the normalization options given by experimental observations of Cosmic Rays (CRs) and photons at different wavelengths. It is essential to discuss in this context which stacking limit can be applied to what prediction. Current neutrino flux limits are investigated in Section 3. A general ansatz for the interpretation of stacking limits as diffuse limits is presented here. In Section 4, the method is applied to AMANDA’s limits which have been derived by stacking AGN according to their electromagnetic output. The question which stacking limits apply to which normalization scenario is discussed in Section 5 and it is examined how the limits constrain different models. In Section 6, further source classes are examined according to the possibility of applying the stacking method for high energy neutrinos, i.e. $E_\nu > \text{TeV}$. In addition, a comparison of the contribution from the northern and southern hemisphere is done for various source classes in order to compare the capabilities of next generation’s telescopes ICECUBE and KM3NET. The results are summarized in Section 7.

2 Discussion of prevailing neutrino flux models

In some hadronic acceleration models it is assumed that for each class of AGN, the electromagnetic emission is correlated to a neutrino signal. Apart from individual normalization factors, the corresponding cosmological integrations are basically mathematically identical. In this section, the correlation between the emission of neutrinos and photons at different wavelengths will be discussed according to neutrino flux models which are currently being discussed in the literature.

2.1 *TeV photon sources and Cosmic Rays*

Sources of electromagnetic TeV emission can be interpreted as optically thin to photon-neutron interactions, $\tau_{\gamma n} \ll 1$ (e.g. Mücke et al., 2003; Mannheim et al., 2001) in hadronic acceleration models. In such a scenario, charged Cosmic Rays (CRs) are produced in the vicinity of the source through the decay of the escaping neutrons. In this case, the resulting neutrino energy density would be proportional to the extragalactic CR component measured at Earth. A theoretical upper bound of such a contribution to the diffuse neutrino flux has been derived by Mannheim, Protheroe and Rachen (in the following referred to as the *MPR bound*), see (Mannheim et al., 2001). Within the framework of the proton-blazar model, the neutrino flux from High-frequency peaked BL Lacs (HBLs) has been calculated using the connection between Cosmic Rays and neutrino emission, see (Mücke et al., 2003).

2.2 Normalization to the diffuse EGRET and COMPTEL spectrum

In the case of optically thick sources ($\tau_{\gamma n} > 1$), the photons interact with nucleons in the source before escaping at lower energies leading to the emission of sub-TeV photons. Therefore, the diffuse extragalactic background determined by the EGRET¹ experiment (Sreekumar et al., 1998; Strong et al., 2005) ($E_{\gamma} > 100$ MeV) can be interpreted as an avalanched TeV signal from blazars and can thus be used to normalize the neutrino flux from EGRET or COMPTEL²-type sources. Again, MPR give an upper bound to the contribution from such sources in (Mannheim et al., 2001), which is much less restrictive than the optically thin case. Apart from the bound, a calculation of the maximum contribution from blazars is given in (Mannheim et al., 2001). In addition to the contribution from HBLs within the framework of the proton-blazar model, a contribution from the optically thick Low-frequency peaked BL Lacs (LBLs) can be calculated using the EGRET diffuse extragalactic background for a normalization of the neutrino spectrum, see (Mücke et al., 2003). A model of $p\gamma$ interactions in AGN and collisions of protons from the core with protons of the host galaxy is derived in (Mannheim, 1995). This model will be referred to as *M95-A*. Alternatively to optically thin sources with photon emission above 100 MeV, the environment can be optically thick allowing only photons below 100 MeV to escape. In that case, the neutrino signal can be normalized to the diffuse extragalactic contribution measured by COMPTEL at energies in the range of (0.8, 30) MeV (Kappadath et al., 1996). This would enhance the contribution of neutrinos from $p\gamma$ by almost an order of magnitude as shown in (Mannheim, 1995). We will refer to this model as *M95-B* in the following.

A model by Stecker & Salamon (1996) was originally using the diffuse cosmic X-ray background (see Sec. 2.3) and has recently been modified in a way that it is using the COMPTEL diffuse background to normalize the neutrino spectrum (Stecker, 2005). This reduces the formerly very high contribution by a factor of 10. In addition, oscillations have been taken into account which leads to a further reduction by a factor of 2.

2.3 The ROSAT X-ray background as normalization option

The measurement of the diffuse extragalactic contribution in X-rays by ROSAT³ has raised the question whether it is produced by radio-weak AGN. Assuming that the X-ray emission comes from the foot of the jet, the X-ray signal

¹ Energetic Gamma Ray Experiment Telescope

² COMpton TELEscope

³ ROentgen SATellite

would be accompanied by a neutrino flux. A model by Nellen et al. (1993) and an approach by Stecker & Salamon (1996) have been presented. An alternative scenario would be the up-scattering of thermal electrons via the Inverse Compton effect. In that case, the X-ray component would not be accompanied by a neutrino signal, see e.g (Mannheim et al., 1995). Until today, about 75% of the diffuse X-ray signal has been resolved by ROSAT (Brandt & Hasinger, 2005), with the help of CHANDRA and XMM⁴-NEWTON data, this number can be updated to 90%, see (Brandt & Hasinger, 2005) and references therein. More than 70% of the diffuse background could be connected to the X-ray emission of Active Galactic Nuclei most of which are radio weak. AMANDA's measurements of a diffuse neutrino flux did not yield a significant signal and constrains these models strongly.

2.4 Correlated radio and neutrino emission

Detailed examination of multi-wavelength observations have shown a correlation between the disk and jet power of Active Galactic Nuclei, see (Falcke et al., 1995; Falcke & Biermann, 1995, 1999). This correlation can be used to determine the diffuse neutrino flux from FR-II galaxies and flat spectrum radio quasars within the framework of the jet-disk symbiosis model (Becker et al., 2005). The neutrino flux has been assumed to follow an E^{-2} spectrum which leads to a relatively high neutrino flux at energies above TeV energies. Assuming on the other hand a correlation between the radio spectral index and the index of the proton spectrum leads to an $E^{-2.6}$ neutrino spectrum. Since the flux is normalized at low energies, the contribution decreases significantly at higher energies with an increasing spectral index.

3 Neutrino flux limits

The conversion of stacking limits into stacking diffuse limits is the main topic of this section. Basically we use the contribution of the identified sources to the integrated background at a chosen electromagnetic wavelength to estimate by way of a physical model the corresponding ratio for neutrinos: What fraction of identified neutrino source candidates goes towards the integrated background? It is important to note here that we use conservative estimates in order to obtain absolute, reliable upper limits. As limits to the flux of identified source classes we use the sample of AGN classes from the AMANDA stacking analysis which is described in (Achterberg et al. (IceCube Coll. & P. L. Biermann), 2006; Achterberg et al. (IceCube Coll.), 2007).

⁴ X-ray Multi-Mirror Mission

To avoid any confusion of the notation, a paragraph on the limit conventions precedes the actual discussion of the limits.

3.1 Limit Conventions

Throughout this paper, several types of neutrino flux limits will appear. Limits are usually given in the form $E^2 \cdot dN/dE$ with dN/dE as the differential neutrino flux at Earth and E as the neutrino energy.

Throughout the paper, the limits will be denoted as follows:

- Φ^{DL} : Diffuse Limit (DL) derived by using data from the complete northern hemisphere. It is given in units of $\text{GeV cm}^{-2} \text{s}^{-1} \text{sr}^{-1}$.
- Φ^{SL} : Stacking Limit (SL) in units of $\text{GeV cm}^{-2} \text{s}^{-1}$, obtained for the point source flux from a certain class of AGN. The principle is indicated schematically in Fig. 1. As an example, three source classes, FR-I and FR-II galaxies as well as blazars, are displayed. The stacking limits are obtained by stacking the most luminous sources of the same class in the sky, indicated by sources with filled circles. Weaker sources (empty circles) are not included.
- Φ^{SDL} : Stacking Diffuse Limit (SDL), derived from the stacking limit in the same units as the diffuse limit, $\text{GeV cm}^{-2} \text{s}^{-1} \text{sr}^{-1}$. It is determined by taking into account the contribution from weaker sources as well as yet unidentified sources, present in a diffuse background.

A similar convention is used to denote the corresponding sensitivities:

- Φ^{DS} : Diffuse Sensitivity (DS), giving the sensitivity of AMANDA towards a diffuse signal from the northern hemisphere. Units are $\text{GeV cm}^{-2} \text{s}^{-1} \text{sr}^{-1}$.
- Φ^{PS} : the sensitivity to a single point source in AMANDA. Units are $\text{GeV cm}^{-2} \text{s}^{-1}$.

3.2 Limits on the total diffuse neutrino flux

The unfolded spectrum of the diffuse neutrino flux as observed by the AMANDA experiment is indicated in e.g. Fig. 8. It can be seen that the measured flux follows the prediction of the atmospheric neutrino spectrum and no extragalactic contribution is observed (Münich et al., 2005). The unfolded spectrum is derived using data from the year 2000. The current limit on the diffuse muon neutrino flux from extragalactic sources is given for four years of data (2000-2004) (Achterberg et al. (IceCube Coll.), 2007),

$$\Phi^{\text{DL}} = 7.4 \cdot 10^{-8} \text{GeV cm}^{-2} \text{s}^{-1} \text{sr}^{-1} \quad (1)$$

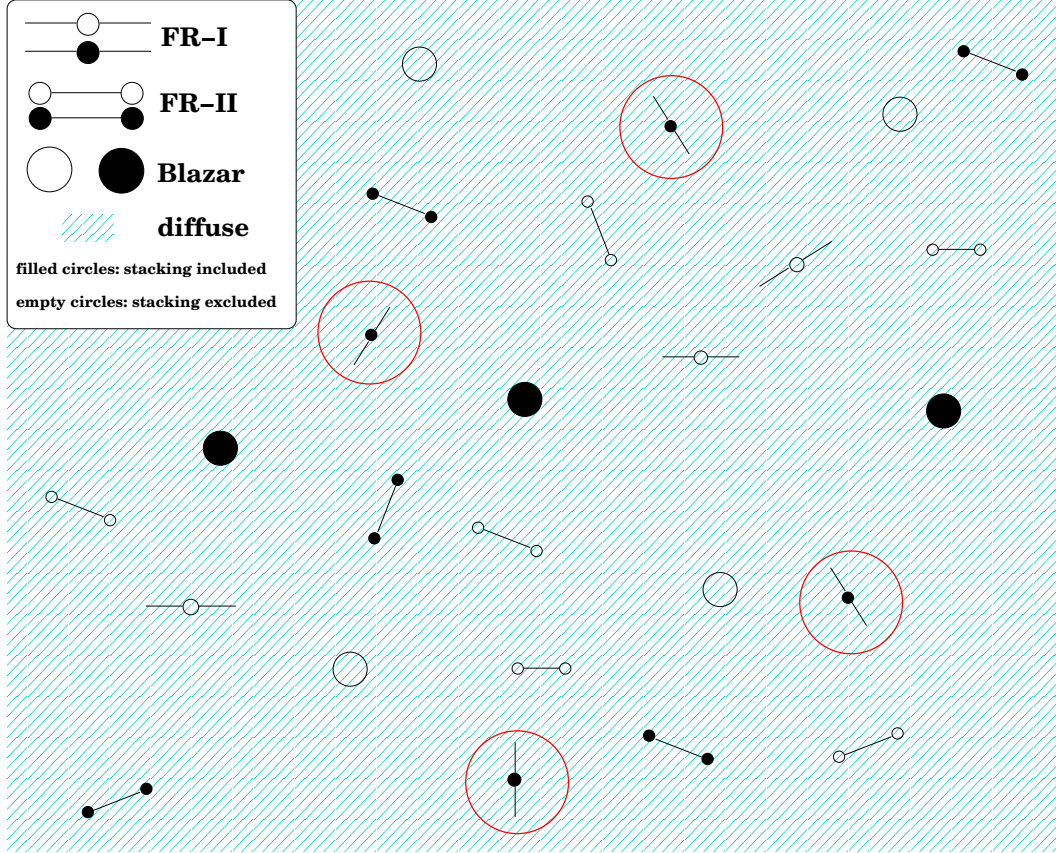


Fig. 1. Schematic figure of the principle of source stacking. Objects are classified into source classes (here: FR-I and FR-II galaxies as well as blazars). Under the signal hypothesis that photons in a certain bandpass are directly correlated to neutrinos, the sources are selected according to their strength in the corresponding bandpass. The most intense sources are then stacked for an analysis of a neutrino signal from the source class. This is indicated for the case of FR-I galaxies as circles around the objects. Only the strongest sources are used in the stacking analysis (filled circles), while weaker objects are not used (empty circles). An estimate of the remaining source signal is needed as well as knowledge about unresolved sources, possibly seen as diffuse background in order to interpret the stacking neutrino limits as diffuse upper bounds to the given source class. The diffuse background varies with the source class.

in the energy range of $10^{4.2}$ GeV to $10^{6.4}$ GeV.

In addition to a diffuse search, AMANDA examines a possible signal from single sources. No signal excess above the atmospheric background was observed yet. To maximize the significance of the signal to background expectation, a stacking method has been applied examining different source classes of AGN (Achterberg et al. (IceCube Coll. & P. L. Biermann), 2006).

This method is commonly used in cases where a single source is not likely to have a significant signal above background (e.g. Mannheim et al., 1996). Given the limit for a certain source class, Φ^{SL} , the differential flux renormalized to a diffuse signal is

$$\Phi^{\text{SDL}} = \epsilon \cdot \xi \cdot \frac{\Phi^{\text{SL}}}{2\pi \text{sr}}. \quad (2)$$

The transition from point source to diffuse flux is done by dividing the source limits by AMANDA's field of view, 2π sr. The stacking factor ϵ is the ratio of the total photon signal in the sample and the photon signal which is included in the analysis. Figure 1 gives a schematic representation. The stacking factor corrects for all sources with empty circles in the diffuse limit, since the signal from these sources is not included in the stacking analysis. The diffusive factor ξ represents the ratio of the total diffuse flux to the contribution of resolved sources. Sources which have not been resolved yet have to be considered as potentially contributing to the total diffuse neutrino signal as they contribute to the isotropic photon signal. In Fig. 1, this is indicated by the diffuse background which is different for each source class. This background is identified in a few cases by looking at the luminosity function of the objects, in others by measurements of the diffuse component. A detailed view on ϵ and ξ will be given in Section 4.

4 Point source limits on AGN neutrino fluxes

Recently, a stacking analysis has been published for the first time for a neutrino signal from Active Galactic Nuclei for which eleven AGN source classes have been defined. The source classes have been defined and selected as follows. The catalogs below have been selected in (Achterberg et al. (IceCube Coll. & P. L. Biermann), 2006).

- (1) GeV blazars detected by EGRET (*GeV*).
- (2) Unidentified GeV sources observed by EGRET (*unidGeV*). Sources of possible galactic origin have been excluded.
- (3) Blazars that have been observed at infrared wavelengths (*IR*).
- (4) Blazars that have been observed at keV wavelengths by the experiment HEAO-A⁵ (*keV(H)*).
- (5) keV blazars observed by the ROSAT experiment (*keV (R)*).
- (6) The class of blazars with observed TeV emission (*TeV*).
- (7) Compact Steep Sources (CSS) and GHz peaked sources (GPS) (*CSS/GPS*) as selected by O'Dea & Baum (1997).

⁵ High Energy Astronomy Observatories-A

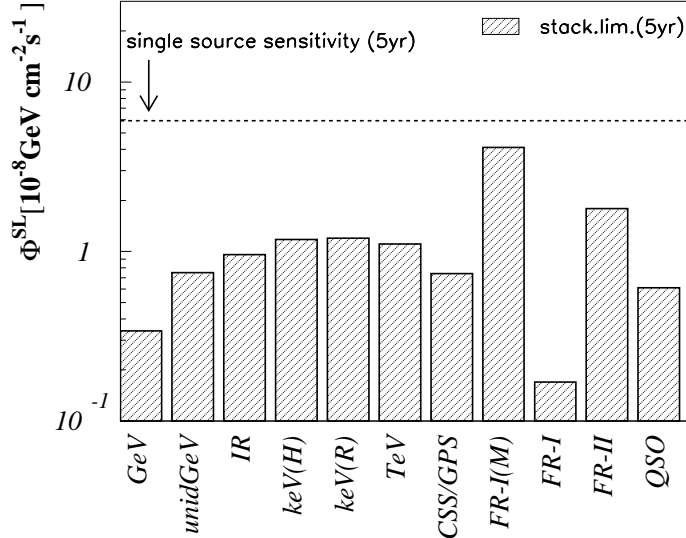


Fig. 2. Limits on the neutrino flux for a given source class. Limits in this representation are given per source. The source classes are labeled with the abbreviation indicated in the list of the samples above.

- (8) Low luminosity Faranoff Riley galaxies (FR-I) with M-87 included (*FR-I(M)*).
- (9) FR-I galaxies excluding M-87 (*FR-I*). These two different cases are necessary to consider, since M-87 is the closest AGN (distance ~ 20 Mpc) and dominates the total signal of all FR-I galaxies.
- (10) High luminosity Faranoff Riley galaxies (*FR-II*).
- (11) Quasi Stellar Objects (*QSO*).

References to the corresponding catalogs as well as a detailed description of the analysis methods are given there. In brackets, the abbreviations for the source classes are given as they appear in Fig. 2.

The limits on the neutrino flux from the given source classes are displayed in Fig. 2. They are compared to AMANDA's single source sensitivity of $\Phi^{\text{PS}} = 5.9 \cdot 10^{-8} \text{ GeV cm}^{-2} \text{ s}^{-1}$ to point out the improvement that has been achieved in the stacking approach. In the following, the stacking factor ϵ and the diffusive factor ξ will be discussed. It will be shown that seven of the eleven samples can effectively be used to determine a diffuse limit on the neutrino flux from the given class.

4.1 The Stacking factor

The number of sources in a sample that is included in the stacking analysis is determined by optimizing the expected significance for signal and background. Subsequently, the amount of the total photon signal of the analyzed sources is determined by the number of included objects. This is shown schematically in Fig. 1. The strongest FR-I galaxies (filled circles) are included in the stacking analysis. The stacking process for FR-I galaxies is indicated by circles around the stacked objects. FR-I galaxies having a too weak signal (empty circles) are not part of the stacking and have thus to be included in the *stacking factor* ϵ . Quantitatively, the ratio of the total photon signal and the signal of the sources that are used in the stacking approach is represented by ϵ . The precise values of ϵ for each class are given in Table 1.

Some of the stacking classes cannot be used for a diffuse interpretation. Firstly, the number of sources needs to be sufficiently high. An indication for an insufficient number of sources would be the use of all the sources in a sample in the stacking analysis. Secondly, the luminosity function should be moderately falling: if only very few sources in our vicinity dominate the signal, no conclusions about the overall diffuse contribution can be justified.

The complete sample was used for stacking in several cases due to the low number of detected sources in the given wavelength interval. In particular, these source classes are the infrared and HEAO-A sources as well as the TeV blazars. Since all twelve observed infrared sources have been used and only three sources are reported from HEAO-A, a diffuse limit to the source class cannot be derived for these samples. There are five sources in the stacking sample of TeV blazars. Due to the small number, this class cannot be used for a diffuse interpretation. Due to the strong absorption of the TeV signal in photons, the contribution of a neutrino flux from TeV-resolved photon sources is expected to be much lower than the total flux. This is discussed in detail in section 5.

Apart from the three classes already excluded, the class of FR-I galaxies including M-87 is not suitable for an interpretation of a stacking limit as a diffuse limit: M-87 makes up most of the photon signal from all FR-I galaxies. This is also the reason why the stacking limit is very close to the single point source sensitivity. This result must therefore rather be interpreted as a point source result of M-87. The FR-I sample without M-87 on the other hand is applicable for the diffuse interpretation.

Source class	selected	ϵ	ξ	Φ^{SL}	possible
	wavelength				diffuse limit?
EGRET GeV	> 100 MeV	1.4	< 12	2.71	yes
unid. EGRET	> 100 MeV	1.3	1	31.7	yes
infrared	60 μm	1	-	10.6	no
keV (HEAO-A)	(0.25, 25) keV	1	-	3.55	no
keV (ROSAT)	(0.2, 2) keV	1.2	1.43	9.71	yes
TeV blazars	> 100 GeV	1	-	5.53	no
CSS/GPS	178 MHz, 2.7 GHz, 5 GHz	1.3	model dep.	5.94	yes
FR-I w. M-87	178 MHz	-	-	4.11	no
FR-I w/o M-87	178 MHz	1.1	model dep.	2.91	yes
FR-II	178 MHz	2.65	< 160	30.4	yes
QSOs	UV	1.3	model dep.	6.70	yes

Table 1

Table of the source class limits obtained with the stacking method. Five years of data, 2000-2004, have been used for the analysis with AMANDA in (Achterberg et al. (IceCube Coll.), 2007). Listed are the source class, the selection wavelength, the stacking and diffusive factors, the stacking limit Φ^{SL} in units of $10^{-8} \text{ GeV cm}^{-2} \text{ s}^{-1}$ and the possibility of interpreting the stacking result as a diffuse limit.

4.2 The diffusive factor

Apart from the contribution of resolved sources to a diffuse background, a component of unresolved sources has to be considered. The ratio of the total diffuse signal to the signal of resolved sources is called the *diffusive factor* ξ in the following. In Fig. 1, this is indicated as the diffuse photon background of unidentified sources. A truly diffuse contribution from e.g. dark matter decays is discussed as a component of the diffuse photon background (Biermann & Kusenko, 2006), but it will be considered as negligible here. Any contribution of a diffuse component not connected to any source population would improve the limits accomplished.

70% of the diffuse X-ray background has been identified as AGN in the ROSAT data sample (Brandt & Hasinger, 2005). Thus, the diffusive factor ξ , which is the inverse of the fraction of resolved sources, for the keV ROSAT data sample is given as $\xi_{\text{ROSAT}} = 1.43$. Note that today, XMM-Newton and CHANDRA provide values of $\sim 95\%$ resolved sources. But since both the

neutrino flux predictions are based on and the stacking limit has been derived from ROSAT data, a fraction of 70% resolved sources is used.

For EGRET sources, it could be shown that only 1/12 of the total diffuse background can be made up by resolved sources, as derived by Chiang & Mukherjee (1998). The claim from Chiang & Mukherjee (1998) that about 25% of the diffuse background of blazars is made up by resolved AGN, while the remaining contribution is from unresolved sources which are not blazars, would reduce ξ significantly to $\xi_{EGRET} \approx 4$. However, Stecker & Salamon (2001) point out that this estimate is based on assumptions that do not hold for EGRET blazars. Thus, $\xi_{\max} = 12$ will be used as a conservative number in the following. With the launch of GLAST⁶, the question of the contribution from resolved blazars will most likely be settled.

For the remaining source classes, there is no explicit estimate of the contribution of resolved sources to a diffuse background. In this case, an estimate of ξ can be possible for source populations where there is an estimate of the weakest sources in the sky. In this case, the luminosity evolution of the population has to be considered. In the Euclidean case, sources evolve as $N(> S) \propto S^{-3/2}$ with S as the observed flux and $N(> S)$ as the number of sources for fluxes greater than S . In such a case, the integral of the distribution diverges for a vanishing minimal source strength, $N(S_{\min} \rightarrow 0) \rightarrow 0$. For cosmological sources, the behavior is not Euclidean and in some cases, it is possible to determine a lower threshold for the flux, see (Longair, 1998, e.g.). For instance, such determination can be done in the case of FR-II galaxies which are high luminous AGN with a defined luminosity limit of $L_{radio} \sim 10^{43}$ erg/s (Faranoff & Riley, 1974).

The determination of a lower luminosity limit enables the calculation of the total number of sources in a population N_{tot} . The total number of sources is given by integrating the number per flux interval, dN/dS over the flux:

$$N_{tot} = \int_{S_{\min}}^{\infty} \frac{dN}{dS} dS. \quad (3)$$

For the case of divergence for $S_{\min} \rightarrow 0$, the lower integration limit is essential to know as mentioned before. This is not trivial, since measurements for most source classes do not reveal the low luminosity cutoff. The luminosity functions of different AGN classes at $z = 0$ are shown in Fig. 3.

In this case, the diffusive factor can be estimated by assuming that sources which are not in the catalog are not stronger than the weakest source in the catalog. Thus, the flux of any additional source S_{add}^i is smaller than the flux

⁶ Gamma-ray Large Area Space Telescope

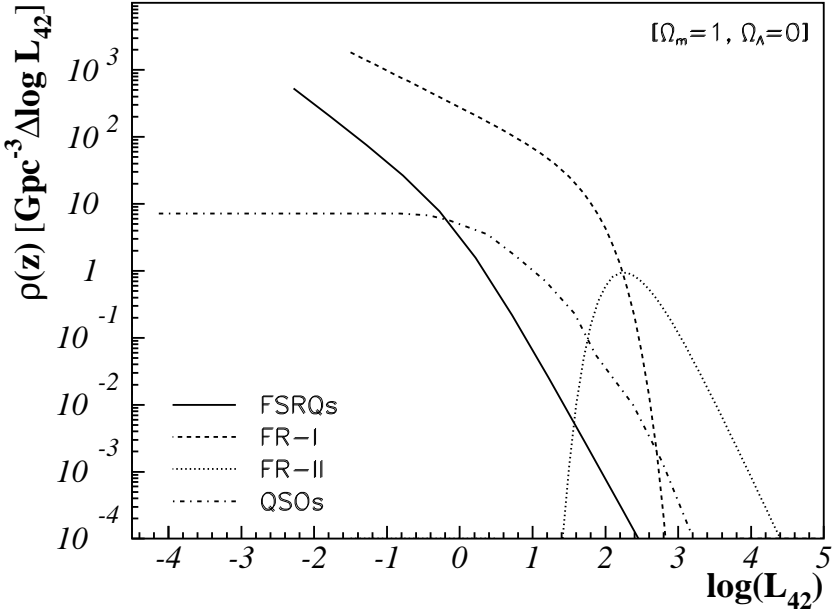


Fig. 3. Radio Luminosity Functions at $z = 0$ for Flat Spectrum Radio Quasars (FSRQs, solid line) (Dunlop & Peacock, 1990), FR-I and FR-II galaxies (dashed and dotted lines) (Willott et al., 2001), as well as for QSOs (dot-dashed line) Schmidt (1972). Density units are $1/\text{Gpc}^3 \cdot \Delta \log L$ and luminosity units are $L_{42} := L/(10^{42} \text{ erg/s})$. Only FR-II galaxies show a cutoff at low luminosities. All other source classes show an increasing or constant population with decreasing luminosity.

of the weakest source, S_{weak} , $S_{add}^i < S_{weak}$ for all non-resolved sources i . The total flux not considered in the calculation is thus

$$S_{tot}^{add} = \int \frac{dN}{dS} S dS < S_{weak} \cdot N_{add}. \quad (4)$$

Here, $N_{add} = N_{tot} - N_{cat}$ is the number of additional sources which is calculated from the total number of sources expected in the sky, N_{tot} , subtracting the number of sources in the catalog, N_{cat} . Then, ξ is calculated to

$$\xi = \frac{S_{tot}^{cat} + S_{tot}^{add}}{S_{tot}^{cat}} \quad (5)$$

$$\xi_{\max} = \frac{S_{tot}^{cat} + S_{weak} \cdot N_{add}}{S_{tot}^{cat}}, \quad (6)$$

where S_{tot}^{cat} is the total flux in the catalog.

Figure 4 shows the behavior of the maximum value of the diffusive factor ξ_{\max} according to Equ. (6) at the example of EGRET sources. The figure emphasizes the challenge in such a representation. It is essential to have an estimate of the total number of sources in the class to get a good estimate for ξ_{\max} . This implies the necessity of the knowledge of the absolute lower luminosity limit. For FR-II galaxies, this is relatively simple, since the number of sources decreases for low luminosities (Willott et al., 2001). FR-I galaxies on the other hand have a high number of low luminosity sources and it is not known at which luminosity the function turns.

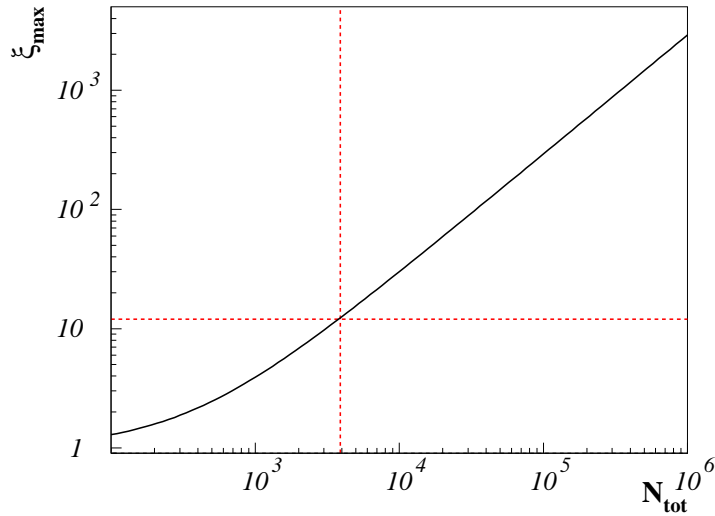


Fig. 4. Maximum diffusive factor ξ_{\max} versus total number of > 100 MeV-emitting sources for EGRET sources. With $\xi_{\max} = 12$, the lower limit of the total number of sources contributing to the diffuse EGRET background is $N_{\text{tot}} > 3.9 \cdot 10^3$.

In such a case, the diffusive factor can be quite large, since a high contribution from low luminosity sources is expected. Thus, ξ has explicitly been determined according to the neutrino flux model which is tested by the limits. For FR-II galaxies, the investigated neutrino flux model presented by Becker et al. (2005) uses the luminosity function by Willott et al. (2001), labeled "FR-II" in Fig. 3. In this case, a total number of $\sim 10^5$ sources is expected and the maximum diffusive factor is determined to $\xi_{\max} = 160$. For the remaining source classes, FR-I galaxies, GPS/CSS and QSOs, the value of ξ_{\max} will not be given, since no explicit neutrino model for these source classes is examined here. Note that ξ_{\max} gives an absolute upper limit: every source not included in the stacking analysis is assumed to have the flux of the weakest included source, S_{weak} . This results in an overestimate of ξ , since it is likely that only a small fraction of the sources has such a high flux.

For EGRET sources, Equ. (6) can be used to determine a lower limit of sources contributing to the diffuse EGRET background. Figure 4 shows the dependence of the maximum value of ξ on the total number of sources in the source class of blazars emitting at > 100 MeV. Using a diffusive factor of $\xi = 12$, the total number of sources contributing to the total diffuse EGRET background is $N_{tot}^{EGRET} > 3.9 \cdot 10^3$.

4.3 Comparing stacking diffuse limits with overall diffuse results

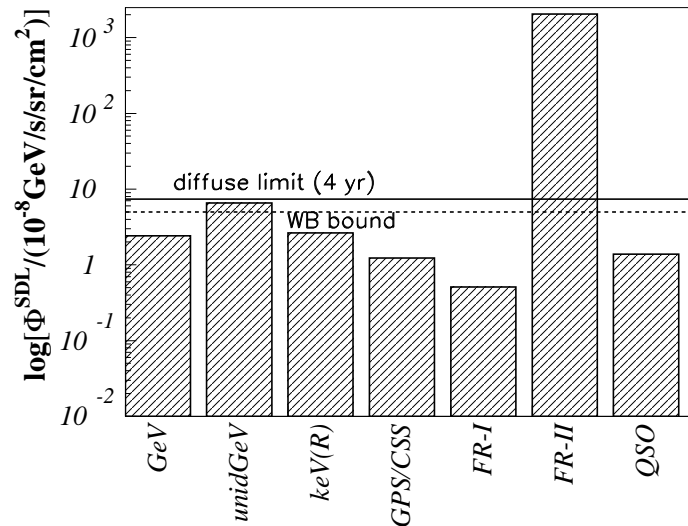


Fig. 5. Diffuse limits of seven different AGN classes. The solid line represents the total diffuse limit of AMANDA (Achterberg et al. (IceCube Coll.), 2007). Several of the stacking diffuse limits are more restrictive than the general diffuse limit. The dashed line indicates the Waxman/Bahcall (WB) bound which gives a theoretical estimation of the maximum contribution of AGN to the diffuse neutrino flux.

Figure 5 shows the diffuse limits that could be derived from the stacking approach for each source class. It is compared to the diffuse limit of AMANDA (solid line) for the operation time considered (2000-2003),

$\Phi^{DL} = 7.4 \cdot 10^{-8} \text{ GeV cm}^{-2} \text{ s}^{-1} \text{ sr}^{-1}$, given in (Achterberg et al. (IceCube Coll.), 2007). Several stacking diffuse limits are more restrictive than the general diffuse limits. The exact numbers are given in Table 2, where the stacking limit, the diffuse bound derived from the stacking method and the ratio of the latter and the general diffuse limit are compared. Note that in the case of CSS/GPS, QSOs and FR-I galaxies, the diffusive factor still has to be applied.

Figure 5 also indicates the Waxman/Bahcall bound (WB bound, dashed line). This bound gives a theoretical estimate of the maximum contribution to be expected in neutrinos from Active Galactic Nuclei (Waxman & Bahcall, 1999). This bound is valid for optically thin sources at an energy of $E_\nu \sim 10^{17}$ eV, where it is most restrictive. The description for all energies is given by Mannheim et al. (2001). Five of the seven source class limits lie below the indicated WB bound. This shows that the sensitivity reached with this method in AMANDA is already extremely high. Next generation's neutrino telescopes such as ICECUBE and KM3NET which will have a cubic kilometer of ice resp. water instrumented will therefore be able to provide more information either by giving very strong restrictions on prevailing models or by confirming a positive neutrino signal.

Note that the class of TeV blazars is on the other hand an optimal candidate for a general diffuse search. The contribution of photon-observable TeV blazars is very small, since many sources are hidden in photons due to the strong absorption, while they would still be visible in neutrinos. This will be discussed in Section 5.

Source class	Φ^{SL}	Φ^{SDL}	$\Phi^{\text{DL}}/\Phi^{\text{SDL}}$	models
EGRET GeV	2.71	7.25	1.02	(Mannheim et al., 2001), (Mannheim, 1995), (Mücke et al., 2003)
unid. EGRET	31.7	6.56	1.23	-
infrared	10.6	EXCL.:	too few	-
keV (HEAO-A)	3.55	EXCL.:	too few	-
keV (ROSAT)	9.71	2.65	2.79	(Stecker & Salamon, 1996), (Nellen et al., 1993), (Alvarez-Muñiz & Mészáros, 2004)
TeV blazars	5.53	EXCL.:	too few*	(Mannheim et al., 2001), (Mücke et al., 2003), (Mannheim, 1995)
CSS/GPS	5.94	$1.23 \cdot \xi_{\text{model}}$	$6.02/\xi_{\text{model}}$	-
FR-I incl. M-87	4.11	EXCL.: M87	dominant	-
FR-I excl. M-87	2.91	$0.51 \cdot \xi_{\text{model}}$	$14.5/\xi_{\text{model}}$	-
FR-II	30.4	$2.05 \cdot 10^3$	$3.61 \cdot 10^{-3}$	(Becker et al., 2005)
QSOs	6.70	$1.39 \cdot \xi_{\text{model}}$	$5.34/\xi_{\text{model}}$	-

Table 2

Table of the source class limits obtained with the stacking method. Five years of data, 2000-2004, have been used for the analysis with AMANDA in (Achterberg et al. (IceCube Coll.), 2007). The stacking limit is given in units of $10^{-8} \text{ GeV cm}^{-2} \text{ s}^{-1}$ while the stacking diffuse limits is given in units of $10^{-8} \text{ GeV cm}^{-2} \text{ s}^{-1}$.

*While the class of TeV blazars cannot be used to determine a stacking diffuse limit, the general diffuse limit gives an upper limit to the contribution of TeV-observable blazars to the total diffuse flux as it is shown in Section 5.

5 Direct implications for AGN neutrino flux models

The diffuse limits discussed in Sections 1 and 4 constrain some of the currently discussed neutrino flux models. However, it is known that these models bear different uncertainties in both normalization and spectral shape due to a lack of knowledge of the conditions at the source.

In this section, the neutrino flux models having been discussed in Section 1 will be examined with respect to the limits obtained.

5.1 *TeV blazars*

The detection of TeV photon emission from distant sources is limited due to the absorption of high energy photons by the extragalactic background light (e.g. Stecker et al., 1992; Kneiske et al., 2004). The absorption factor η describes the ratio of the total emitted TeV photon flux from HBLs and the TeV flux from HBLs up to a redshift z_{\max} . It is a measure of the absorption of TeV photons. The ratio of a diffuse neutrino signal from photon-observable TeV blazars will be calculated using the general diffuse limit and taking into account the absorption factor for TeV photons: Only a relatively small fraction of all TeV blazars can be identified in TeV photons, since sources at high redshifts are hidden due to the strong absorption.

In this paragraph, the absorption factor and the general diffuse neutrino limit are used to derive the maximum contribution of TeV photon-observable sources to the total diffuse neutrino flux.

5.1.1 *The absorption factor η*

In the case of TeV blazars, the absorption factor η is much greater than unity due to the strong absorption of TeV photons by the extragalactic background light. HBLs seem to have no or even a slightly negative evolution (e.g. Beckmann et al., 2003; Bade et al., 1998; Laurent-Muehleisen et al., 1999).

For a no-evolution scenario as it is discussed for BL Lacs, the co-moving density $\rho(z)$ is considered to be constant with redshift, $\rho(z) = \text{constant}$. Using a negative evolution with less than $(1 + z)^{-0.2}$ does not change the results significantly. We also neglect the positive source evolution which has to be present up to a certain redshift z^* : both effects positive evolution up to z^* and negative evolution at higher redshifts are believed to cancel. Each effect for itself alters the result less than 10% in opposite directions.

The normalization of the co-moving density is not important in this calculation, since only ratios of concrete values of ρ are considered and the constant of proportionality cancels.

The neutrino flux from sources up to a certain redshift z_{\max} is given by

$$\frac{dN}{dE} = \phi_0 \cdot \int_{z=0}^{z_{\max}} E'(z)^{-2} \cdot \rho(z) \frac{dV_c}{dz} dz, \quad (7)$$

where $E'(z) = (1+z) \cdot E$ is the energy of the neutrino at the source. The E^2 -weighted flux is thus given as

$$E^2 \frac{dN}{dE} = \phi_0 \cdot \zeta(z_{\max}). \quad (8)$$

Here, $\zeta(z_{\max}) = \int_{z=0}^{z_{\max}} (z+1)^{-2} \cdot \rho(z) dV_c/dz dz$ is the evolution factor depending on the upper redshift integration limit z_{\max} . If all present sources are considered, $z_{\max} \approx 7$ is a reasonable value. Recent searches for luminous galaxies at redshifts between $z = 6 - 8$ imply that only few ultra-luminous objects only exist beyond $z = 7$ (Iye et al., 2006; Bouwens & Illingworth, 2006). At higher redshifts, no large galaxies are observed, leading to the conclusion that only smaller galaxies can be present. Also, the results do not change significantly when going up to higher redshifts: the major contribution comes from redshifts of $z < 3$.

The absorption factor η is given by the ratio of the total flux and the contribution that is observed by TeV-photon experiments:

$$\eta(z_{\max}) = \frac{\zeta(7)}{\zeta(z_{\max})}. \quad (9)$$

Here, z_{\max} is the maximum redshift at which TeV photon sources can be identified by present Imaging Air Cherenkov Telescopes (IACTs). TeV sources have up to today been observed up to a redshift of $z=0.186$ - 1ES1101-232 (Aharonian, 2006). As a conservative upper limit, the maximum redshift of observation with IACTs is taken to be $z_{\max} = 0.3$, since an upper bound is derived from these values. The absorption factor depending on z_{\max} is shown in Fig. 6. At $z_{\max} = 0.3$, the numerical value is

$$\eta(z_{\max} = 0.3) = 54. \quad (10)$$

It is important to note that for a lower energy threshold (e.g. 30 GeV), IACTs could be able to detect sources up to $z_{\max} \sim 1$. This would lead to a much

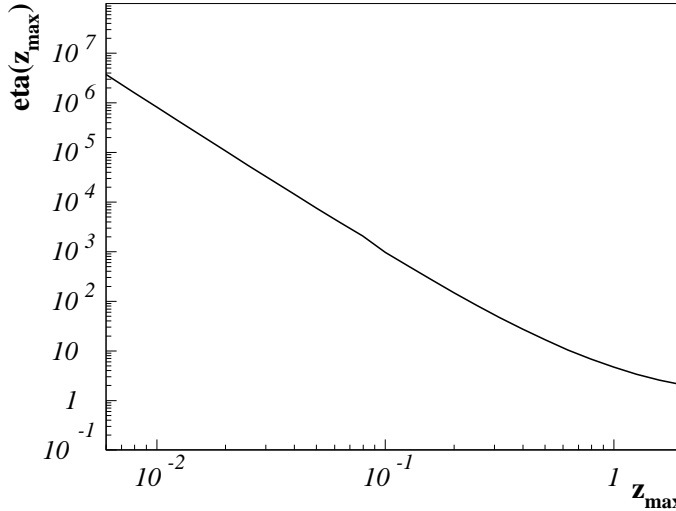


Fig. 6. Absorption factor η versus maximum redshift z_{\max} . For TeV sources, the most distant source observed is 1ES1101-232 at $z=0.186$ (Aharonian, 2006). $\eta(z_{\max} = 0.3) = 54$ is used for TeV sources.

lower absorption factor of

$$\eta(z_{\max} = 1) = 4.6. \quad (11)$$

5.1.2 An upper limit to the contribution from photon-observable TeV blazars

Using the above reflections, one can argue that a diffuse limit can be used to estimate the maximum diffuse signal from HBLs resolved in TeV photons: From the existing general diffuse limit, it is known that no source type and, thus particularly also not the class of TeV blazars, can contribute more than $\Phi^{\text{DL}} = 7.4 \cdot 10^{-8} \text{ GeV cm}^{-2} \text{ s}^{-1} \text{ sr}^{-1}$:

$$E^2 \frac{dN}{dE} \Big|_{\text{TeV}} < \Phi^{\text{DL}}. \quad (12)$$

An upper limit to the normalization constant ϕ_0 of the neutrino flux can be derived by inserting Equ. (8) with $z_{\max} = 10$ in Equ. (12):

$$\phi_0 < \frac{\Phi^{\text{DL}}}{\zeta(10)}. \quad (13)$$

The contribution of sources at $z < z_{\max}$ is given as

$$E^2 \frac{dN}{dE} \Big|_{TeV} (z_{\max}) = \phi_0 \cdot \zeta(z_{\max}) < \frac{\zeta(z_{\max})}{\zeta(10)} \Phi^{\text{DL}} \quad (14)$$

with the final result of

$$E^2 \frac{dN}{dE} \Big|_{TeV} (z_{\max}) < \eta(z_{\max})^{-1} \cdot \Phi^{\text{DL}}. \quad (15)$$

The upper limit on the neutrino flux up to z_{\max} is shown in Fig. 7. The curve shows the no-evolution scenario.

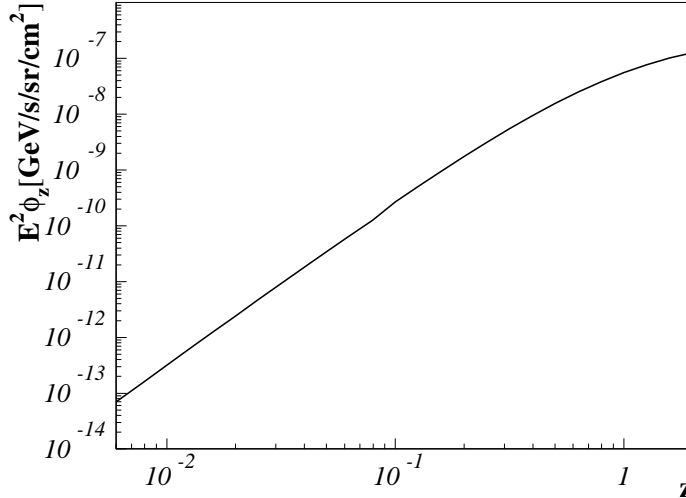


Fig. 7. Upper limit on the contribution of photon-observable TeV blazars for the no-evolution scenario for HBLs.

The contribution of photon-observable TeV blazars to the diffuse neutrino flux is therefore limited to

$$E^2 \frac{dN}{dE} \Big|_{TeV} (z_{\max} = 0.3) < 1.37 \cdot 10^{-9} \text{ GeV cm}^{-2} \text{ s}^{-1} \text{ sr}^{-1}, \quad (16)$$

where $\eta(z_{\max} = 0.3) = 54$ is used as a lower limit. The contribution of sources observed by IACTs is thus about three orders of magnitude lower than the possible total contribution. This is displayed in Fig. 8 together with the general diffuse limit. The limit to the maximum contribution from photon-observable TeV blazars is shown (*obs. TeV*) as well. The contribution is a factor of $\eta^{-1} \approx 0.019$ lower than the diffuse limit. This indicates that a diffuse analysis of

TeV sources is most effective with an overall diffuse approach, since most of the TeV sources are hidden due to the strong absorption at such high photon energies. The stacking of the strongest sources in the sky in comparison only comprise a small fraction of the total diffuse flux as these calculations show. This result stands in contrast to the other sources samples where the selection of the strongest sources yields stronger restrictions than a general search for a diffuse signal, see following paragraphs.

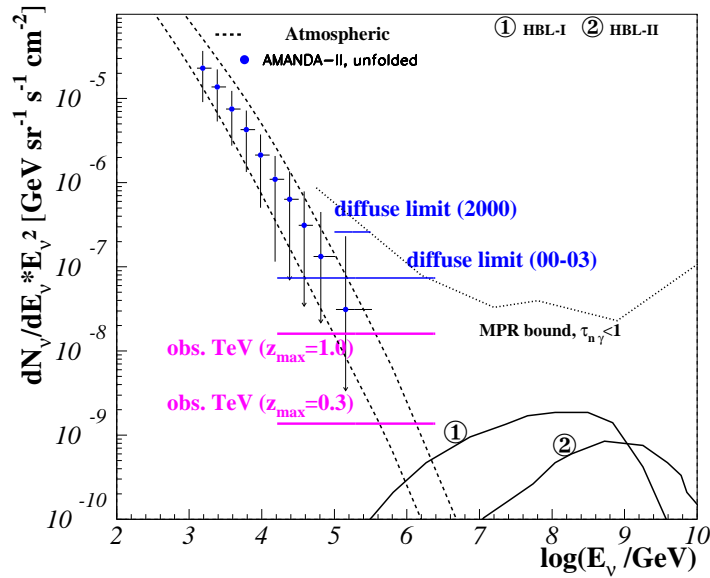


Fig. 8. Neutrino predictions for optically thin sources. TeV photons from decaying pions escape together with neutrons which make up charged CRs by decaying in the vicinity of the source in protons. All models have been corrected for oscillations. The *MPR-bound* derivation is described in (Mannheim et al., 2001). Predictions for the contribution from HBL sources (*HBL-I* and *HBL-II*) depend on the extension of the acceleration region and the jet frame target photon density. Model 1 and 2 represent two different parameter settings, see (Micke et al., 2003). The general diffuse limit is shown as well as the limit to photon-observable TeV blazars (*obs. TeV*), indicating that the major contribution to the diffuse neutrino signal from TeV blazars is expected to come from hidden TeV photon sources for two different maximum redshifts, $z = 0.3$ and $z = 1$.

The importance of reaching down to low energies with IACTs is demonstrated in this calculation, since lowering the energy threshold to observe sources up to $z = 1$ would already include sources with a one order of magnitude higher

maximum neutrino flux of

$$E^2 \frac{dN}{dE} \Big|_{TeV} (z_{\max}) < 1.60 \cdot 10^{-8} \text{ GeV cm}^{-2} \text{ s}^{-1} \text{ sr}^{-1}. \quad (17)$$

5.2 Optically thick cases: sources of MeV and GeV γ emission

If the sources are optically thick to photon-neutron interactions, $\tau_{\gamma n} \gg 1$, the photon signal which is emitted from the sources lies in the MeV to GeV range. Thus, EGRET and COMPTEL diffuse cosmic photon fluxes are used to determine the expected neutrino contribution.

5.2.1 EGRET blazars

Figure 9 shows neutrino flux predictions in connection with EGRET data and the derived stacking diffuse limits for a neutrino signal from EGRET sources. Since the indicated models are all normalized to the EGRET diffuse spectrum, the limit of identified EGRET blazars applies. The gray line between 1 TeV and $10^{2.8}$ TeV indicates the most conservative calculation where it is assumed that the total diffuse background as measured by EGRET is produced by AGN ($\xi = 12$). The limit falls short of the MPR bound and also touches the maximum prediction for the source class predicted by MPR and it is possible to reach sensitivities at the level of predictions concerning a neutrino signal from blazars. The same is valid for the prediction by Mannheim (M(95), A): The proton-proton contribution from optically thick blazars can be constrained even though the atmospheric flux exceeds the prediction at these energies. With an overall diffuse analysis, it would not be possible to extract any information on this low-energy part of the spectrum from AGN.

The contribution from LBL within the proton-blazar model dominates the total observable flux at ultra high energies. With the current data, it is not possible to get to any reliable conclusion from the stacking method, since it is valid at energies $E < \text{PeV}$ while the flux is present at much higher energies. A stacking analysis of cascade events with second generation telescopes such as ICECUBE would be an option to explore regions of energies at $> \text{PeV}$. A stacking approach for cascades is however accompanied by the challenge of getting a reasonable directional reconstruction of the neutrino events, since the cascade signal is generally not as boosted as a signal from neutrino-induced muons.

Even in the most conservative case of a diffusive factor of $\xi_{\max} = 12$, the model of proton-proton energies can be constrained at low energies. With the stacking method, the diffuse limit can be extended to sensitivities far below

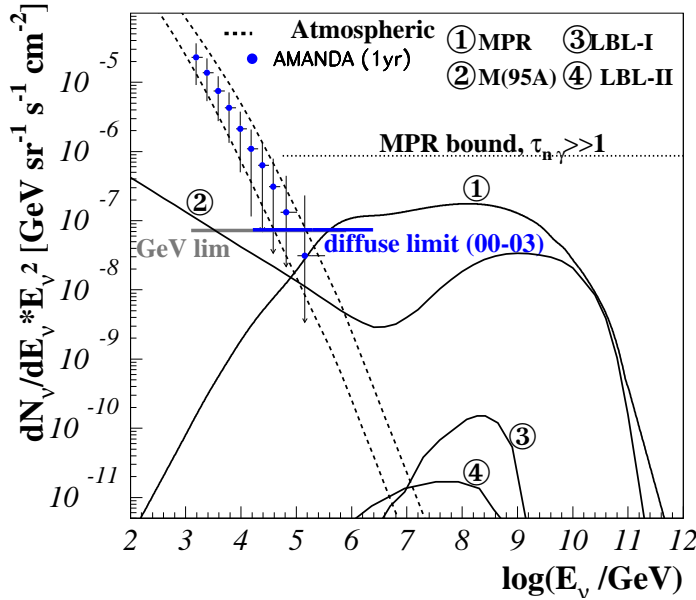


Fig. 9. Neutrino flux predictions for optically thick sources, normalized to the diffuse EGRET flux above 100 MeV. Model 1 (*MPR*) represents the maximum contribution from blazars within the framework of Mannheim et al. (2001) in which the *MPR bound* for optically thick sources (dashed line) is derived. Model 2 (*M95,A*) - gives the neutrino spectrum from $p\bar{p}$ and $p\gamma$ interactions in blazars determined in Mannheim (1995). Models 3 and 4 (*LBL-I* and *LBL-II*) represent the prediction of neutrinos from LBLs given two different parameter settings, see Mücke et al. (2003). The stacking diffuse limit for the class of identified EGRET sources is indicated with $\xi = \xi_{\max} = 12$ where it is assumed that AGN produce the complete diffuse EGRET signal.

the flux of atmospheric neutrinos.

5.2.2 COMPTEL blazars

A stacking analysis using COMPTEL blazars has not been done yet. The option is discussed in Section 6. Current diffuse neutrino flux limits are still about a factor of 2 or more above the predictions. The hypothesis of an avalanched TeV signal down to MeV energies will be tested by ICECUBE.

5.3 The diffuse X-ray background and Radio Weak AGN

The X-ray component of radio weak AGN can be correlated to the emission of neutrinos at the foot of the jet. This has been investigated in calculations of Nellen et al. (1993), Stecker & Salamon (1996) as well as Alvarez-Muñiz & Mészáros (2004). All models are constrained by the current general diffuse AMANDA limit. The resolved ROSAT sources which have been used to determine the stacking limit are radio loud and thus, the limit is not as easily applicable to these predictions. If the same production mechanism is assumed in radio loud as in radio weak sources, the stacking diffuse limit of ROSAT sources would apply in this case.

However, the limit to radio weak objects Φ^{SDL}_{rq} is about a factor of 10 higher than the calculated limit for radio loud sources Φ^{SDL}_{rl} , since radio loud objects are about a factor of 10 less frequent than radio weak sources,

$$\Phi^{\text{SDL}}_{rq} \lesssim 10 \cdot \Phi^{\text{SDL}}_{rl} = 1.72 \cdot 10^{-7} \text{ GeV cm}^{-2} \text{ s}^{-1} \text{ sr}^{-1}.$$

The more restrictive limit in this case is therefore the general diffuse limit.

Figure 10 shows the prediction of neutrinos being produced coincidentally with X-rays at the foot of AGN jets. The diffuse ROSAT-measured background has been used in two models (Nellen et al., 1993; Stecker & Salamon, 1996) to normalize the neutrino spectrum. In the third case presented by Alvarez-Muñiz & Mészáros (2004), the luminosity evolution function of radio quiet AGN has been used so that the result also applies to the correlation with the X-ray diffuse background.

In the case of the prediction by Nellen et al. (1993), AMANDA's diffuse neutrino flux limit lies an order of magnitude below the flux. Stecker et al. updated their calculation by normalizing to the diffuse flux as measured by COMPTEL (Stecker, 2005). This is discussed in the context of the MeV photon emission in correlation with neutrinos in Section 5.2. The absence of neutrinos from ROSAT-detected sources implies strongly that the X-ray emission from AGN cannot be directly correlated to neutrino emission. While the missing emission of neutrinos disfavors a hadronic scenario for the X-ray emission from AGN, it is consistent with Inverse Compton (IC) models for the X-ray emission and underlines leptonic models for the production of X-rays in AGN.

Calculations by Stecker & Salamon (1996) show a flux peaking at higher energies compared to the prediction from Nellen et al. (1993). The main reason is that Nellen et al. (1993) use a more conservative estimate of the maximum energy and a simpler approach for the spectral behavior. The spectrum of the model by Stecker & Salamon (1996) is not exactly E^{-2} -shaped, while

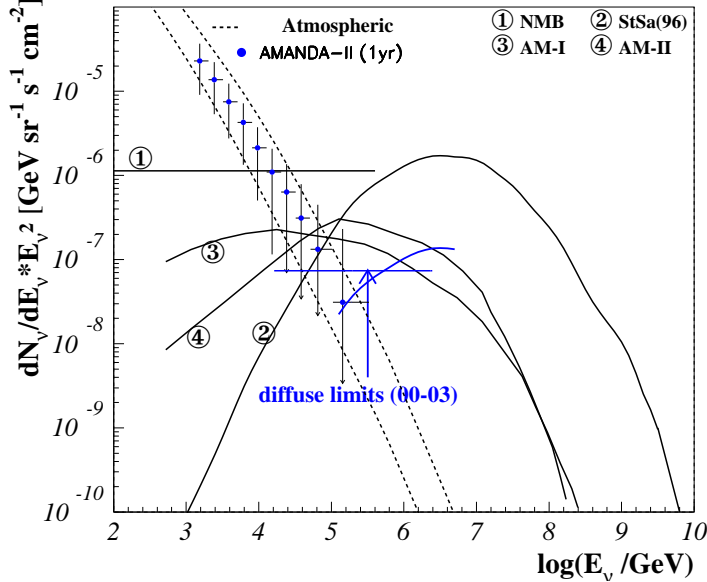


Fig. 10. Stecker & Salamon (1996) (*StSa96*, model 2) predict a large contribution of neutrinos from radio weak sources using ROSAT data to normalize the spectrum. Nellen et al. (1993) (*NMB*, model 1) use the same normalization method. Model 3 and 4 (*AM-I* and *AM-II*, (Alvarez-Muñiz & Mészáros, 2004)) use the luminosity function of radio quiet AGN and normalize the single source spectrum. While the black hole mass is varied in model 3, model 4 varies the accretion rate. All these models have been corrected for neutrino oscillations. All models are excluded in their published form by AMANDA's diffuse limit. The typical E^{-2} limit is represented by the blue horizontal line. The curved blue line, crossing the E^{-2} -limit represents the AMANDA limit for the years 2000-2003 calculated for a flux shaped as the model by Stecker & Salamon (1996) and Stecker (2005).

the AMANDA limits are typically derived assuming an E^{-2} spectrum. The modeling of different spectral shapes, including Stecker & Salamon (1996), has been done recently, see (Hodges et al., 2006). The curved blue line indicates the limit modeled according to the model of Stecker & Salamon (1996). The limit lies half an order of magnitude below the prediction.

While the previously described models normalize the diffuse spectrum by using ROSAT data, calculations by Alvarez-Muñiz & Mészáros (2004) use the radio luminosity function for radio quiet AGN and a single source normalization. Further differences with respect to model 1 and 2 are the maximum energy and the break in the neutrino spectral shape. The underlying idea is the same by assuming proton-proton and proton-photon interactions at the foot of AGN jets, leading to X-rays in coincidence with neutrinos. This model overproduces neutrinos as well as the previous ones.

Three independent calculations on the correlation of X-ray emission from radio quiet AGN and neutrino emission have been examined. The absence of neutrino emission from the foot of relativistic jets implies that the particles there are not accelerated to high energy, and then interact. However, the concept that the innermost ring of the accretion disk, just underneath the jet, turns into an Advection Dominated Accretion Flow (ADAF) with a very high temperature (e.g. Falcke et al., 1995; Biermann et al., 1995; Rachen et al., 1995; Donea & Biermann, 1996; Mahadevan, 1998), is consistent with the results. This implies that the spin parameter of the black hole is high, above 0.95, and that hadronic interaction at weakly relativistic temperatures produce charged pions, which decay and provide an energetic particle seed population for further acceleration downstream for the radio emission of the jet (Gopal-Krishna et al., 2004). This is then consistent with an Inverse Compton explanation of the X-ray emission (Mannheim et al., 1995), and predicts that there should be a large production of energetic neutrinos at an energy commensurate with the pion mass.

5.4 Radio galaxies

The radio emission of Active Galactic Nuclei is likely to be directly correlated to neutrino emission in the jet. This has been discussed by Becker et al. (2005) at the example of FR-II radio galaxies and flat spectrum radio quasars (FSRQs). In both cases, the normalization of the neutrino spectrum depends on many different intrinsic factors, i.e. the correlation between radio and disk luminosity and the parameterization of the maximum proton acceleration energy. The jet-disk correlation of AGN has been worked out by Falcke et al. (1995); Falcke & Biermann (1995, 1999). Although the model includes several parameters, all are fixed by the comparison with the data except the accretion rate. Within that model, it is shown that the parameter reach extreme values and are not strongly scattered. The jet-disk symbiosis model has been proven for different source types, reaching from microquasars to quasars.

A parameter in the calculation of the neutrino flux is the optical depth of the source which is unknown. In (Becker et al., 2005), the effective optical depth of the source, τ_{eff} is defined as product of the proton-photon optical depth $\tau_{p\gamma}$ and a reduction factor due to contributions from Bethe-Heitler production η' ,

$$\tau_{eff} = \tau_{p\gamma} \cdot \eta'. \quad (18)$$

It can be derived from the solution of the transport equation, the neutrino flux is proportional to $\tau_{eff}/(1 - \exp(-\tau_{eff}))$. For large depths, the neutrino flux is therefore proportional to τ_{eff} . The effective optical depth has been chosen to

be $\tau_{eff} = 1$ in the calculations described above. The optical depth of proton-photon interactions is determined by the product of the photo-hadronic cross section $\sigma_{p\gamma}$ and the photon density in the source, n_γ . These in turn depend on the disk luminosity L_{disk} and the extent r of the source such as

$$\tau_{p\gamma} = 800 \frac{L_{46}}{r_{17}}, \quad (19)$$

with $L_{46} := L_{disk}/10^{46}$ erg/s and $r_{17} := r/10^{17}$ cm. This shows that the photo-hadronic optical depth itself uncertain, since low values around unity are possible as well as extremely high numbers. AMANDA limits will be used to derive limits on the optical depth of FR-II galaxies and FSRQs.

Note that the determination of τ_{eff} happens only within the specific model of neutrino production as it is described above. The difficulty of drawing more general conclusions lies in the uncertainty of the spectral index. This highly depends on the original spectral behavior of the protons. This can only be simulated and is not directly observable.

5.4.1 FR-II radio galaxies

Using a generic E^{-2} spectrum for the neutrino flux from FR-II galaxies, the flux normalization has been derived to be

$$\Phi = 1.43 \cdot 10^{-7} \text{ GeV cm}^{-2} \text{ s}^{-1} \text{ sr}^{-1}. \quad (20)$$

Comparing the normalization in Equ. (20) with the diffuse limit shows that a flux with the chosen parameter settings is not detected. An upper limit to the optical depth can be derived from the limit yielding

$$\tau_{eff} < 0.5. \quad (21)$$

Within three years of ICECUBE, it will be possible to explore sources with $\tau_{eff} > 0.029$.

Figure 11 shows the prediction of a neutrino flux from FR-II radio galaxies. Model (1) is the original calculation of Becker et al. (2005) modified by a factor $\tau_{eff}=0.5$. This is the maximum contribution for an E^{-2} signal from those sources not violating the diffuse limit of AMANDA. However, there is another production scenario which leads to a significant reduction of a contribution from FR-II galaxies. The synchrotron spectral index of FR-II galaxies α is correlated to the neutrino spectral index p by $p = 2 \cdot \alpha + 1$ (Rybicki & Lightman, 1979, e.g.). The mean synchrotron spectral index is

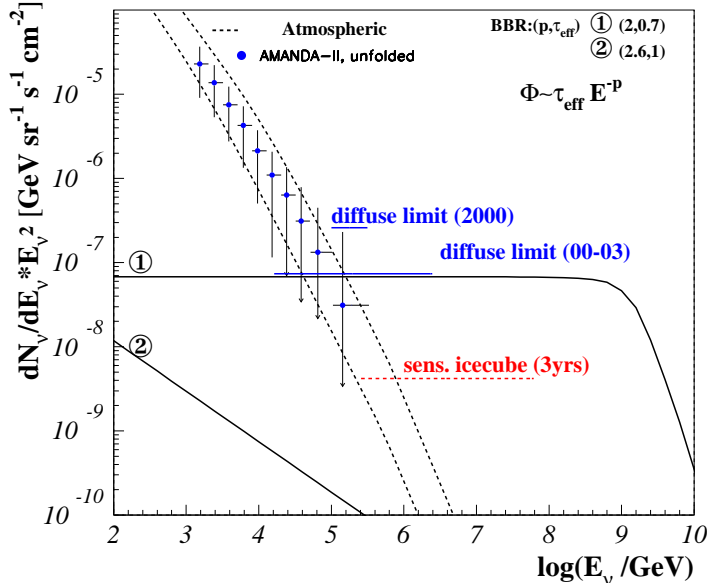


Fig. 11. Contribution to the diffuse neutrino background from FR-II radio galaxies. For an E^{-2} spectrum, it is constrained to an optical depth of $\tau_{eff} < 0.5$. A steeper spectrum $E^{-2.6}$ (model 2) is consistent with the current limit.

$\alpha \approx 0.8$ for large scale emission and therefore, the neutrino spectrum can be as steep as $E^{-2.6}$. This prediction is shown in Fig. 11 as model (2). In that case, the contribution is very low and does neither violate the current diffuse limit, nor is it within reach of ICECUBE's sensitivity for three (or even five) years of operation (Achterberg et al. (IceCube Coll.), 2007). In such a case, an observation of a neutrino signal from FR-II galaxies would be very difficult. If the spectrum were this steep for real, then all Ultra High Energy Cosmic Ray (UHECR) arguments would fail and so it may be more appropriate to assume a flatter spectrum. The radio spectral index of the hot spots are usually about $\alpha \sim 0.6$ and so correspond to a particle spectral index of about $p \sim 2.2$. Using Fig. 11 it can be estimated that a spectrum with an index of 2.2 could already be explored by the three year sensitivity of ICECUBE.

5.4.2 Flat Spectrum Radio Quasars

Using a similar correlation between radio and neutrino flux as for FR-II galaxies, the contribution from FSRQs to the diffuse neutrino flux can be calculated to

$$E^2 \frac{dN}{dE} = 1.70 \cdot \tau_{eff} 10^{-9} \text{ GeV cm}^{-2} \text{ s}^{-1} \text{ sr}^{-1}. \quad (22)$$

The flux lies well beyond the current diffuse limit and even below the sensitivity of ICECUBE for an optical depth around $\tau_{eff} = 1$. Equivalent as for the case of FR-II radio galaxies, the upper limit to the optical depth in FSRQs can be determined to be

$$\tau_{eff} < 44 \quad (23)$$

by using the diffuse AMANDA limit.

The effective optical depth is quite uncertain in the case of Flat Spectrum Radio Quasars. Just as an example, a sub-class of FSRQs are GPS, which are compact AGN where it is assumed that the jet runs into dense matter, yielding a high potential for proton-photon interaction which results in a high optical depth. However, other sources like TeV blazars contribute to the source class, being at the other end with a very low optical depth.

With ICECUBE, it will be possible to examine sources with $\tau_{eff} > 2.5$. Consequently, neutrino emission in coincidence with the radio signal from FSRQs will only be observable in the near future, if the optical depth of FSRQs is significantly higher than the one for FR-II galaxies.

6 Examination of source class capabilities

In the previous sections it has been shown that the stacking method can be used to increase the diffuse sensitivity of high energy neutrino telescopes to certain source classes.

Further catalogs published recently which are not yet part of the stacking search in AMANDA will be discussed in this section. The references for the catalogs are given throughout the text. They will be examined with respect to the potential neutrino signal and the effectiveness of the method.

Also, a diffuse component from unresolved sources is expected to show deviations from a purely isotropic flux, since it is expected to follow the source distribution in the sky. The total signal from a certain source class to be observed by a neutrino telescope is highly dependent on the detector's field of view. We will generically examine source classes concerning the total flux from the northern respectively from the southern hemisphere. This gives a qualitative examination of the capabilities of ICECUBE and KM3NET which is planned to observe the southern hemisphere. The local supercluster for example is observable from the northern hemisphere and so in some cases, a significant fraction of the total flux in a sample comes from that hemisphere. It is shown, however, that there are classes with the dominant contribution in

the southern sky. A further constraint is the limitation of the source catalogs themselves: radio data are mainly given for the northern hemisphere and there are only a few southern identified sources in the case of very sensitive radio-selected samples. Here, high energy photon catalogs which are mostly provided by satellite experiments are much more complete in the sense of directionality.

6.1 Additional source catalogs

This subsection gives an overview of four additional source catalogs which yield high capabilities for neutrino searches with the stacking approach. The point source sensitivity is likely to be increased in all the cases, diffuse limits can be derived in two of the cases. A summary of the basic properties of these catalogs is given in table 3. The maximum diffusive factor for the examined catalogs can be determined as described in Section 4, Equ. (6), assuming that the total number of sources in that class can be determined. This is quite challenging, since a lower luminosity limit is difficult to determine. Figure 12 shows the increase of the diffusive factor with N_{tot} for the whole sky for all four examined catalogs. Table 4 reviews the parameters used for the four catalogs.

Catalog	energy range	Reference	Underlying ν model
COMPTEL	< 100 MeV	(Kappadath et al., 1996)	(Mannheim, 1995; Stecker, 2005)
INTEGRAL	hard X-ray	(Beckmann et al., 2006)	-
INTEGRAL	soft γ -ray	(Beckmann et al., 2006)	-
Starburst	FIR	-	(Waxman & Bahcall, 1999)

Table 3

Summary of source catalogs interesting to examine with respect to the neutrino output of the sources.

6.1.1 Sources of MeV emission

Neutrino flux predictions using the diffuse background as measured in hard X-rays by COMPTEL are based on the assumption that the cosmic diffuse photon flux below 100 MeV is directly correlated to the neutrino flux. About 10 blazars could be resolved by COMPTEL underlining the assumption that intrinsically weaker AGN are responsible for the diffuse signal. No neutrino stacking analysis of the resolved COMPTEL blazars has been done yet. Using the same assumptions as Mannheim (1995) (*M95-B*) and Stecker (2005) (*StSa05*) would challenge such an analysis. The derivation of a diffuse limit from a stacking limit would however be difficult at this stage, since only a neg-

Catalog	#(sources)	S_{tot}^{cat}	S_{weak}
	south/north		
COMPTEL	11	$0.638 \times 10^{47} \text{ erg/s/Gpc}^2$	$0.0199 \times 10^{47} \text{ erg/s/Gpc}^2$
	5/6	0.326/0.311	0.0384/0.0199
INTEGRAL	15	$175 \times 10^{-11} \text{ erg/s/cm}^2$	$0.98 \times 10^{-11} \text{ erg/s/cm}^2$
(hard X-rays)	10/5	130.08/45.1	0.98/4.34
INTEGRAL	42	$441 \times 10^{-11} \text{ erg/s/cm}^2$	$0.85 \times 10^{-11} \text{ erg/s/cm}^2$
(soft γ rays)	23/19	265/176	1.31/0.85
Starburst	199	17000 mJy	0.906 mJy
	46/153	2260/9480	1.52/0.906

Table 4

Summary of the main parameters in the source catalogs. The total number of sources in a catalog is given, $\#(\text{sources})$. S_{tot}^{cat} is the integrated flux in the catalog and S_{weak} is the measured flux of the weakest source in the sample. Units are given for each individual source class. The second row for each class shows the same properties for north and south (south/north).

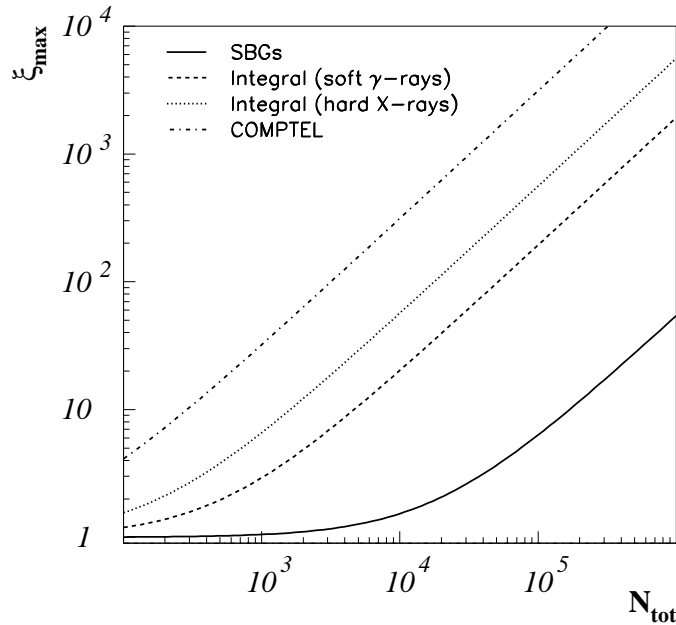


Fig. 12. Behavior of the maximum diffusive factor with the total number of sources in the source class. Only a fraction of the total number of sources is included in the catalog, dependent on the instrument's sensitivity.

ligible fraction of the sources potentially responsible for a diffuse signal is resolved into sources. Thus, the major fraction of the diffuse signal would not be included in a stacking analysis and the limit would not apply to diffuse predictions. The planned launch of satellites such as GLAST (Gehrels & Michelson, 1999) and MEGA⁷ (Kanbach et al., 2004) encourages to pursue the examination of this source class, since it gives the prospect of increased statistics of resolved sources in the considered energy range.

6.1.2 Soft and hard X-rays

As mentioned before, the limit to a neutrino flux from ROSAT-detected sources would be improved significantly by selecting radio-weak sources instead of radio strong ones. A significant neutrino flux would not be expected as discussed in Section 5, but the improvement of the limit would underline the fact that X-ray emission from the foot of the jet is not correlated with a neutrino signal.

In hard X-rays, 15 sources have been identified in the INTEGRAL⁸ survey by JEM-X (Beckmann et al., 2006) and could be interesting to examine. With the current analysis, HEAO-A results were used, while the more recent measurements by INTEGRAL are bound to be more accurate. Since a direct correlation between hard X-ray sources as detected by Integral and soft X-ray sources as seen by ROSAT does not seem to exist, an independent analysis would be reasonable. The emission of hard X-rays is likely to be correlated with TeV photon emission at least via the up-scattering of synchrotron photons by Inverse Compton scattering. Therefore, under the assumption of a correlated emission of hard X-rays and TeV photons, an analysis of the hard X-ray signal gives an indication of the flux from high-frequency peaked BL Lacs.

6.1.3 Soft γ -rays

A catalog of 42 AGN with emission in soft γ -rays, (20, 100) keV has been released by INTEGRAL (Beckmann et al., 2006). Here, some of the sources detected by OSSE⁹ in the energy range of (50, 150) keV could be confirmed, others were not seen. We suggest to use INTEGRAL data to define a source class for the stacking of potential neutrino sources.

⁷ Medium Energy Gamma-ray Astronomy

⁸ INTErnational Gamma-Ray Astrophysics Laboratory

⁹ Oriented Scintillation Spectrometer Experiment

6.1.4 Starburst Galaxies

The emission of neutrinos from Starburst Galaxies has been suggested by Loeb & Waxman (2006) (L&W in the following). It is assumed that

- (1) Relativistic protons are accelerated along with relativistic electrons,
- (2) the observed radio emission results from pion-induced electrons. The same pions produce neutrinos,
- (3) protons lose all their energy in $p\gamma$ interactions before reaching the diffusion time.

It has been pointed out by Stecker (2007) that L&W overestimate the fraction of the diffuse far infrared (FIR) flux coming from Starbursts. While it is $\sim 23\%$ on average, L&W assume that 100% of the detected signal comes from Starbursts. On the whole, the diffuse flux from Starbursts is presumably much lower than predicted: L&W assume that Starbursts are loss dominated, which means that most primaries interact and do not escape the source. This enhances the neutrino flux, since basically all protons lose their energy in $p\gamma$ or pp interactions and produce neutrinos. Observations of the spectral radio index of the sources ($\sim \nu^{-0.8}$) indicate however that Starbursts are in the diffusion limit, indicating that a negligible fraction of protons interact and only few neutrinos are produced. This contribution cannot be expected to be observed by ICECUBE.

There is another possibility to expect enhanced neutrino emission from Starbursts. In the past few years, it could be shown that long GRBs are typically connected to the explosion of Wolf-Rayet stars into a supernova Ic. These occur preferably in Star Forming Regions. Thus, a diffuse flux of GRBs similar to the prediction of Waxman & Bahcall (1999) should originate from the direction of these galaxies. There are two different ways to normalize the diffuse GRB spectrum. One method is to assume that the observed keV-photon flux is proportional to the neutrino flux. In that case, the normalization is dependent on the number of observed GRBs per year. This number is strongly dependent on the instrument and the number is not very exact. Under the assumption that GRBs accelerate protons up to the highest energies, $E_p \sim 10^{21}$ eV, the neutrino spectrum can also be normalized to the flux of ultra high energy cosmic rays (UHECRs). In this case, the normalization is independent of GRB observations. It should be kept in mind that the spectral index of the spectrum still varies from burst to burst - in the model of Waxman&Bahcall, an average spectral index has been used.

It is possible to look for a neutrino signal from GRBs by stacking Star Burst Galaxies. This method has one advantage over a triggered-GRB search: it is a systematic search, since independent of GRB data. A disadvantage is that only nearby events are included, since the sample of Starbursts only reaches

out to redshifts of $z = 0.07$. It should however be possible to use IRAS¹⁰ data to identify Starburst Galaxies at higher redshift. The search for a GRB signal from Starbursts should be considered as a systematic search for choked and undetected GRBs. The sources can be selected according to their FIR-flux, since this is a measure of the SN rate in a Starbursts. A higher FIR flux indicates a high star formation rate, thus more SNe and therefore, also more GRBs.

6.1.5 General approach to optimize stacking for diffuse interpretation

In order to get diffuse limits from source stacking, it is important to choose source classes which have information on both resolved sources and diffuse background. That way, the parameters ϵ and ξ are easily and correctly determined. A good example is the EGRET catalog, where both diffuse and resolved emission could be proven to be correlated. Alternatively, the determination of an upper limit to ξ is possible when working with a relatively complete catalog of the strongest sources in the sky by using a generic number of total sources in the source class as it is described in Section 4, Equ. (6). The diffuse interpretation of source classes like TeV blazars on the other hand is difficult, since IACTs can barely look for diffuse emission and the sensitivity of all-sky monitors such as MILAGRO¹¹ is not high enough yet to detect extragalactic diffuse emission. Future Projects like HAWC¹² experiment as a successor of MILAGRO (Sinnis et al., 2005; Smith et al., 2006) and CTA¹³ following in the footsteps of H.E.S.S.¹⁴ and MAGIC¹⁵, but aiming at a large field of view (Teshima, 2006, e.g.), will help enhancing the completeness of the sample.

In the first approach of AGN stacking in order to examine a potential excess in neutrinos, the number of used sources was determined by optimizing the significance in the detector. The optimal number of sources was in that case typically around ~ 10 . In order to achieve the best stacking diffuse limit it is interesting to optimize the number of sources by taking into account ξ as well. It needs to be tested if, by reducing ξ as much as possible and taking the penalty of a possibly increased point source stacking limit instead, the diffuse limit can be increased. Also, it needs to be considered carefully if an optimization to a possible detection or to a limit is the most reasonable choice.

¹⁰ **I**nfra**R**ed **A**stronomical **S**atellite

¹¹ **M**ultiple **I**nstitution **L**os **A**lamos **G**amma **R**ay **O**bservatory

¹² **H**igh **A**ltitude **W**ater **C**herenkov

¹³ **C**herenkov **T**elescope **A**rray

¹⁴ **H**igh **E**nergy **S**tereoscopic **S**ystem

¹⁵ **M**ajor **A**tmospheric **G**amma **I**maging **C**herenkov **T**elescope

6.2 Source class evolution

For the standard analysis of muon neutrino signatures in high energy neutrino detectors, the field of view is 2π sr. The two experiments ICECUBE and KM3NET will be observing the northern respectively the southern hemisphere in the near future and whole sky coverage is achieved by the combination of the two experiments.

Previously, in the stacking analysis of AMANDA data, sources with $\delta < 10^\circ$ were excluded due to the decreasing sensitivity and high muon background towards the horizon. Here, we include all sources, for both northern and southern hemisphere down to $\delta = 0^\circ$, expecting a much better sensitivity and better muon rejection near the horizon for both ICECUBE and KM3NET due to improved directional reconstruction.

In this section, the different source classes discussed above will be examined with respect to their luminosity evolution. The total sample will be compared to the contribution from the northern and from the southern sky. For each sample, two figures will be discussed. (a) represents the differential source counts, $\log N(> S)$ versus the logarithm of the flux S . (b) shows the integral source evolution with the total flux of N sources, organizing the sources according to their strength, starting with the brightest one. Open (black) sources display in both cases the whole sky. Red stars consider only the southern hemisphere and blue triangles show the northern hemisphere contribution.

6.2.1 Optically thick blazars - MeV to GeV emission

Figure 13 shows the luminosity evolution of EGRET sources, for the whole sky as well as for the northern and southern populations. The three most luminous sources in the EGRET sky are in the southern hemisphere. That is why the main contribution from GeV γ rays is located in the southern hemisphere where the neutrino signal contribution is thus expected to be much higher. Given the restrictive limit which could already be derived from AMANDA data, this source sample is interesting for ICECUBE. Considering the source distribution in the sky, the class of GeV blazars is particularly useful for KM3NET given the high total flux.

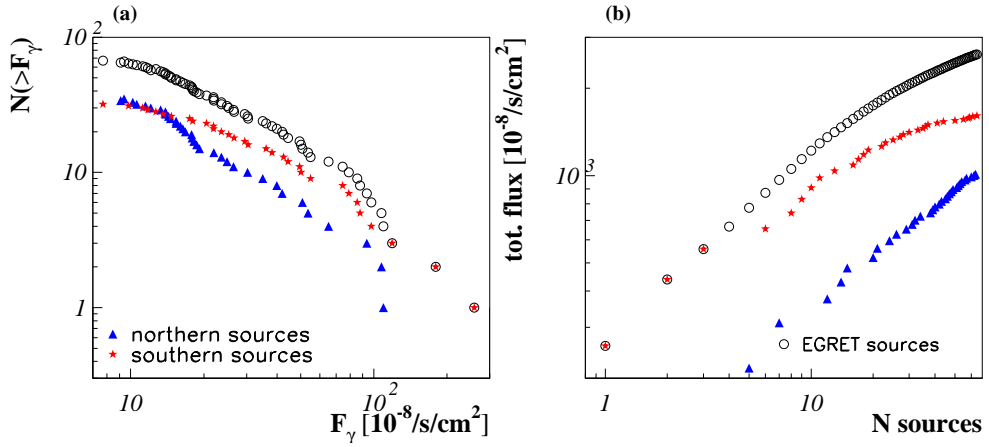


Fig. 13. (a): Number of sources in the EGRET catalog with a flux $> F_\gamma$. The complete catalog is shown as open circles. The sample has been divided into a sub-class of sources at the northern (triangles) and southern (stars) hemisphere. (b): Total luminosities of all sources $< N$, starting to sum up with the strongest source and successively adding the next luminous source.

The COMPTEL Catalog of sources with $E < 100$ MeV is displayed in Fig. 14. In this case, the main contribution lies in the northern hemisphere. The small number of only 11 identified COMPTEL sources make a diffuse interpretation of a possible limit difficult. Satellites like MEGA would make the investigation even more interesting. The 11 identified sources are however still useful to investigate with respect to a point source signal. The maximum diffusive factor lies around $\xi_{\max} \sim 300$ for 10,000 sources and $\xi_{\max} \sim 3000$ for 100,000 sources in the class. Depending on the steepness of the evolution function, this factor can be significantly smaller, so that doubling the number of sources could already help to draw a conclusion about a diffuse limit.

6.2.2 Soft γ -rays

A catalog of soft γ -ray-detected AGN is given by INTEGRAL (Beckmann et al., 2006). 19 of 42 sources are in the northern sky, among the 23 southern sources are the three most luminous ones. The catalog is a good candidate for diffuse interpretation of the neutrino results, given the relatively high number of sources. The luminosity evolution is displayed in Fig. 15. It can be seen that the evolution is still rising and that there is still a significant fraction of signal missing. This is mirrored in the numerical value of the maximum diffusive factor which is calculated to $\xi_{\max} \sim 20$ for $N_{tot} = 10,000$ sources and $\xi_{\max} \sim 200$ for $N_{tot} = 100,000$ sources. These relatively large numbers increase a potential limit on the neutrino flux from INTEGRAL sources by about one order of magnitude¹⁶.

¹⁶ In Section 4 it is already discussed that even with a source class of 10^5 sources, the strongest 10^4 AGN make up the dominant contribution. Thus $\xi_{\max} = 20$ is the

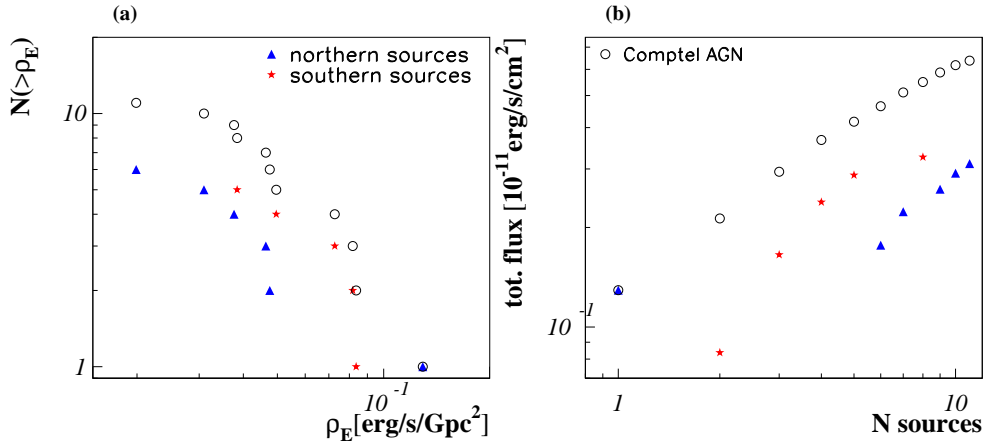


Fig. 14. (a): Number of sources in the COMPTEL catalog with an energy density $> \rho_E$. (b): Total energy density of all sources $< N$, starting to sum up with the strongest source and successively adding the next luminous source.

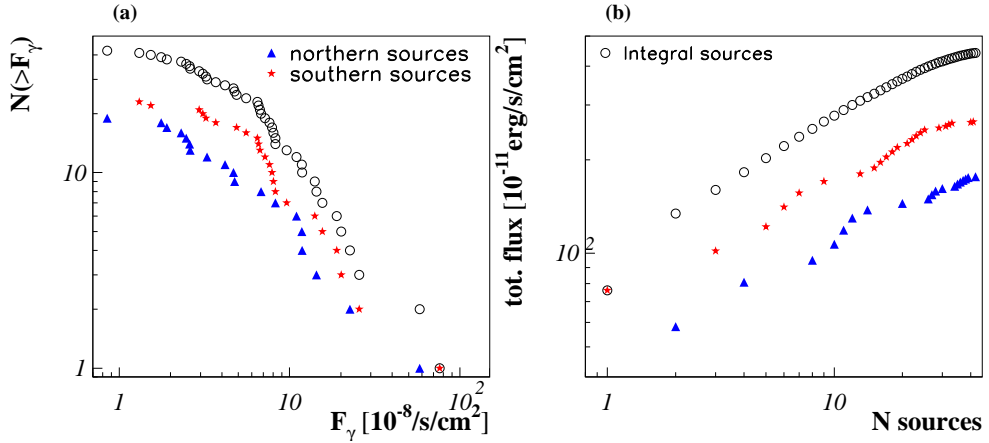


Fig. 15. (a): $\log N(> S) - \log S$ -plot for INTEGRAL sources - total catalog (circles), only northern sources (triangles) and only southern sources (stars). (b): Integral flux versus number of contributing sources.

6.2.3 Soft and hard X-rays

Figure 16 shows the luminosity evolution for ROSAT-detected sources. 84 sources are in the sample totally, of which 35 are northern and 49 are southern sources. The three most luminous sources are in the northern hemisphere.

more realistic value in this case.

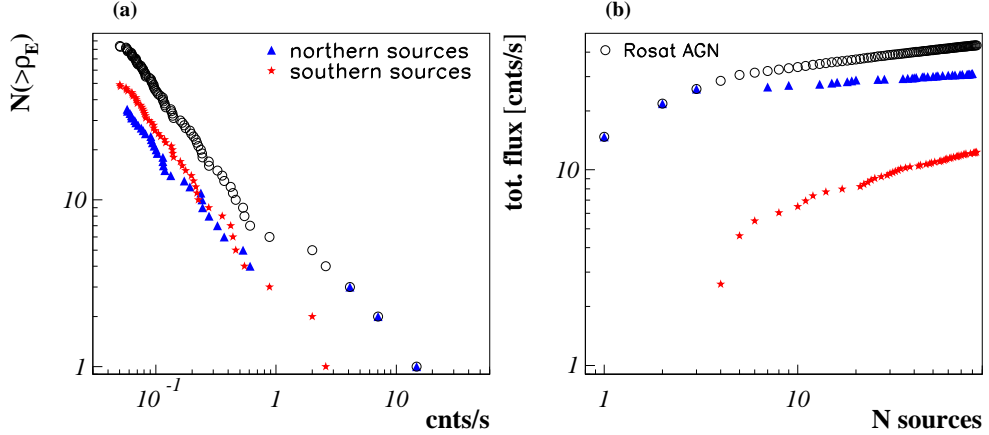


Fig. 16. (a): Number of sources in the ROSAT catalog with an energy density $> \rho_e$. (b): Total energy density of all sources $< N$, starting to sum up with the strongest source and successively adding the next luminous source.

However, these are objects which have such a large flux, since they are extremely close to Earth and not because of their high intrinsic luminosity. This is why these sources were excluded in the stacking analysis of Achterberg et al. (IceCube Coll. & P. L. E. (2006)). Without these sources, the contributions from both hemispheres are comparable.

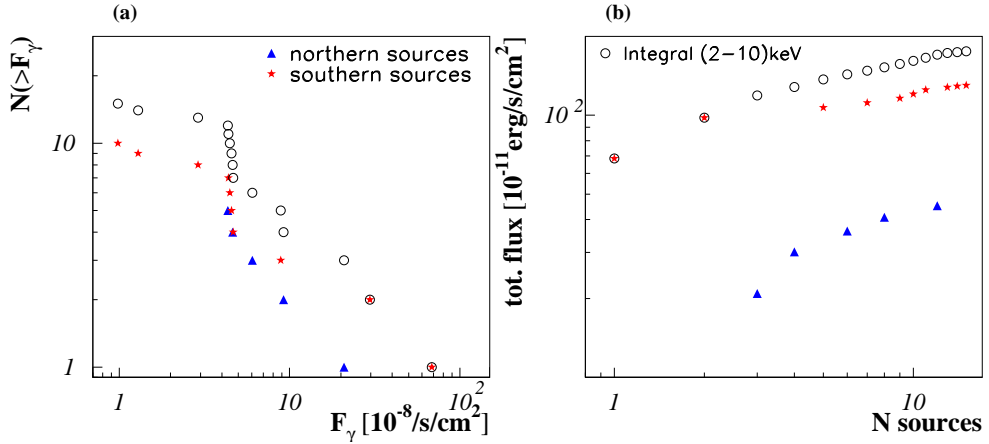


Fig. 17. (a): $\log N(> S) - \log S$ -plot for INTEGRAL sources in hard X-rays (2, 10) keV - total catalog (circles), only northern sources (triangles) and only southern sources (stars). (b) total flux of N contributing sources, starting with the brightest sources and going to weaker fluxes with higher N .

A sample of hard X-ray AGN is available from the INTEGRAL satellite, see Fig. 17. INTEGRAL detected 15 sources in the energy band of 2 keV to 10 keV. Among the 10 sources in the southern hemisphere are the two strongest sources in the sample. There are only 5 northern sources and the main contribution comes from the southern hemisphere. The INTEGRAL sample can improve the stacking analysis of hard X-ray sources which has been done with HEAO-A information. Only three northern sources were reported from HEAO-A. For a diffuse interpretation, there are still too few sources in the sample, though.

6.2.4 FR-I/FR-II

The catalog FR-I and FR-II sources is restricted to values of $\delta > -10^\circ$. Therefore, only few southern sources (7 FR-I and 14 FR-II galaxies) are in the complete sample which is seen in Fig. 18 for FR-I galaxies and in Fig. 19 for FR-II galaxies. The flux is totally dominated by the northern hemisphere.

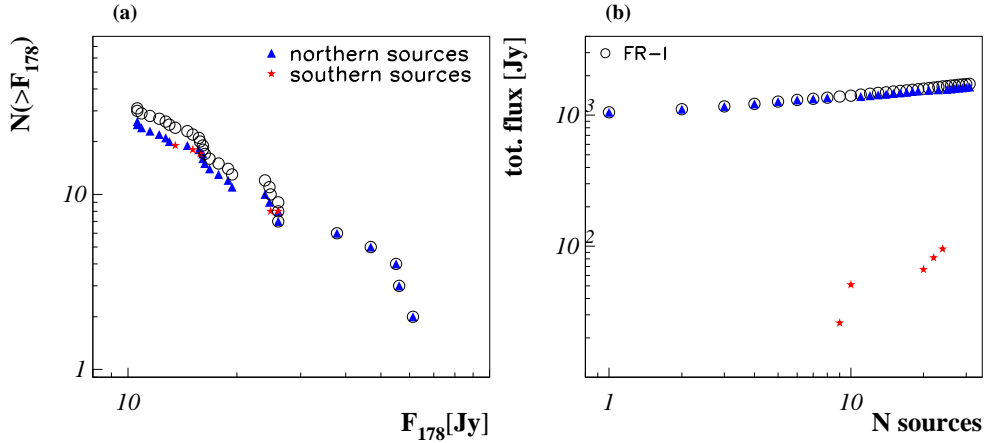


Fig. 18. (a): Number of sources $> S$ for FR-I galaxies. (b) Total flux versus number of sources N .

6.2.5 CSS/GPS

The problem for the catalog of CSS and GPS sources is similar to the situation of the FR-I and FR-II catalog. CSS have been selected at $\delta > 10^\circ$, while GPS include data with $\delta > -25^\circ$. Therefore, there are no southern sources in the case of CSS. Figure 20 shows the GPS sample. 8 southern and 20 northern sources have been identified with the main contribution from the northern hemisphere.

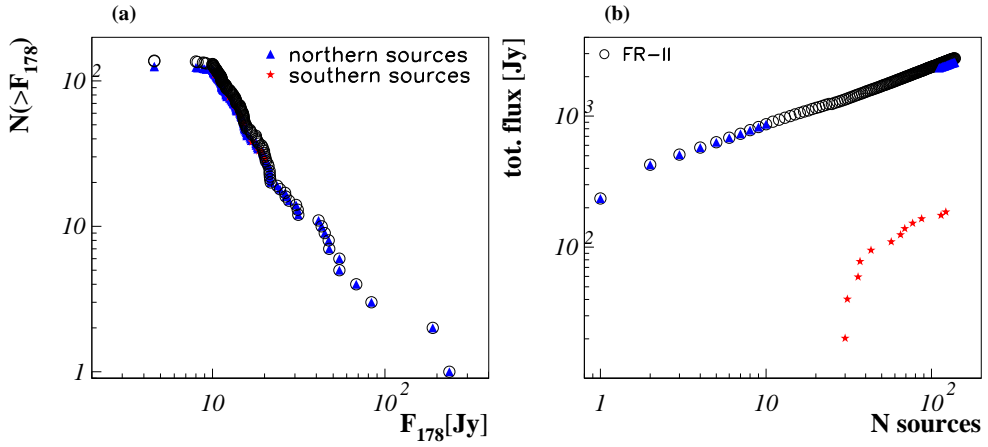


Fig. 19. (a): Number of sources $> S$ for FR-II galaxies. (b) Total flux versus number of sources N .

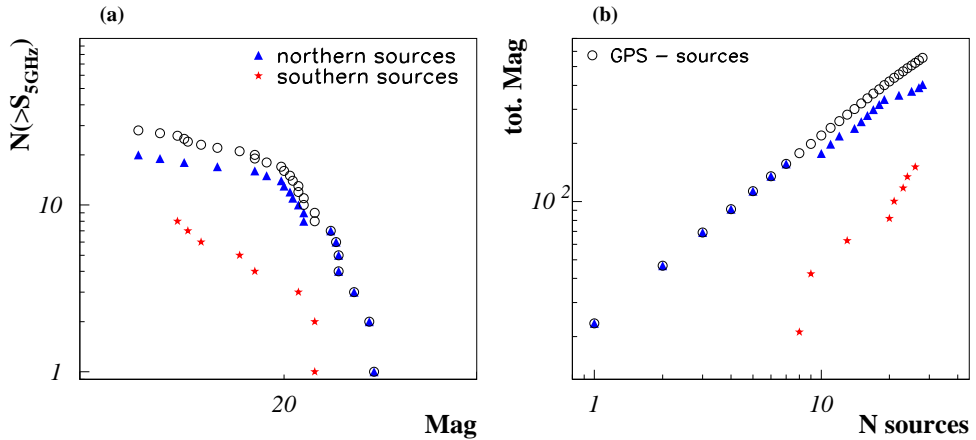


Fig. 20. Giga-Hertz-Peaked Sources (GPS)(O'Dea & Baum, 1997), (a) is the differential flux evolution, (b) shows the total flux versus number of sources N .

6.2.6 QSOs

In the sample of QSOs as presented by Sanders et al. (1989), there are only 3 sources in the southern hemisphere with a measured flux at the selection wavelength, $60\ \mu\text{m}$. The sample selection of the sample was done for $\delta > -15^\circ$, which only leaves a small window on the southern sky. While this source class is well-suited for the analysis of the northern hemisphere, there is too little data available in the southern hemisphere.

6.2.7 Starburst Galaxies

The catalog of Starburst Galaxies includes 199 sources. While the most luminous sources are in the southern, the total flux is higher in the northern hemisphere, since 153 of 199 sources are located north. A stacking analysis has good potential for both hemispheres.

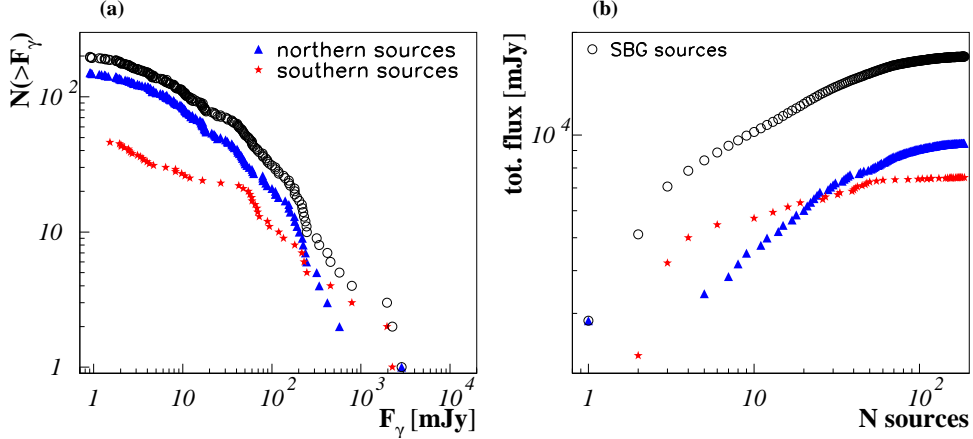


Fig. 21. (a): Number of sources in the Starburst catalog with a flux $> F_\gamma$. (b): Total flux of all sources $< N$, starting to sum up with the strongest source and successively adding the next luminous source.

7 Conclusions and Outlook

In this paper, limits to the diffuse flux from seven different AGN source classes could be derived from point source stacking limits from AMANDA. There is in many cases an additional constraint on flux models at the lowest energies: while the general diffuse limit is restricted to the energy band of $10^{4.2}$ GeV to $10^{6.4}$ GeV, the stacking limits reach down to 10^3 GeV. In many cases, the diffusive factor can conservatively only be estimated. It is expected, that the additional diffuse component is much smaller than the values derived here as upper limits. A reduction of the diffusive factor would result in the improvement of the stacking diffuse limits.

Neutrino flux predictions normalized to the diffuse EGRET signal above 100 MeV use the assumption that the diffuse component is produced by unresolved AGN, see (Mannheim et al., 2001; Mannheim, 1995; Mücke et al., 2003). Thus, the EGRET stacking limit applies to such calculations. The limit falls short of the outline of two of the models, (Mannheim et al., 2001;

Mannheim, 1995). The model of proton-proton interactions normalized to the EGRET diffuse results violates the limit at low energies around 10^3 GeV. At the highest energies, the stacking diffuse limit is more restrictive than the general diffuse limit and reaches below sensitivities of the maximum contribution from proton-photon interactions. A detection of a flux from optically thick blazars should be visible with second generation neutrino telescopes such as ICECUBE.

The neutrino flux models from X-ray detected AGN and from FR-II galaxies can be constrained by the general diffuse limit.

In the case of X-ray AGN, the limit strongly disfavors a hadronic model. It is an order of magnitude below the flux predictions. According to the strongly restrictive limit, neutrinos are not produced at the foot of AGN jets in coincidence with X-rays. Thus, the diffuse emission as measured by ROSAT is likely to be due to Inverse Compton radiation.

Analyzing the correlation between the radio and neutrino emission from FR-II galaxies and blazars, the limit was used to constrain the optical depth of the sources. For FR-II galaxies, $\tau_{eff} < 0.5$ could be derived, while the upper limit for blazars is given as $\tau_{eff} < 44$. Thus, the detection potential for such a source class in ICECUBE is very high, since within three years, ICECUBE is sensitive to sources of optical depth with $\tau_{eff} > 0.024$ (FR-II) resp. $\tau_{eff} > 2.1$ (blazars).

It was shown that a general diffuse analysis gives a high discovery potential for hidden TeV sources: While TeV photons are absorbed at high redshifts, neutrinos propagate freely. An upper limit to the neutrino flux from photon-resolved TeV blazars is determined to be

$$\Phi_{resolvedTeV}^{DL} = 1.37 \cdot 10^{-9} \text{ GeV cm}^{-2} \text{ s}^{-1} \text{ sr}^{-1}. \quad (24)$$

The considerations above show that an investigation of a neutrino signal can be used to help determining different intrinsic parameters of the source type considered. It could be shown that a stacking analysis yields valuable information on the diffuse contribution from these sources. The detection probability is enlarged significantly in such an approach and there is a high detection potential with ICECUBE and KM3NET. A cascade stacking analysis by these neutrino detection arrays should be considered in order to increase the sensitivity to ultra high energy neutrino fluxes as they are described by Mücke et al. (2003).

Apart from the catalogs which have already been used in the stacking analysis of AMANDA, further source classes are investigated here. The possibility of a stacking analysis of COMPTEL sources is discussed in this paper as

a first approach to examine optically thick sources with photon emission of $E < 100$ MeV. Although no stacking diffuse limit can be derived yet due to the small percentage of resolved sources, future experiments such as GLAST at an energy range of (0.02, 300) GeV (Gehrels & Michelson, 1999) and MEGA at (0.4, 50) MeV (Kanbach et al., 2004) give hope to resolve many more sources in the MeV range. Another interesting source class is the catalog of Starburst Galaxies. With the correlation between starforming regions and long duration gamma ray bursts, an enhanced neutrino signal from Starbursts can be expected. The prospects of ICECUBE and KM3NET are different considering source stacking. Most catalogs show a bias to one of the hemispheres. Both neutrino detection arrays can be used to extract complementary information about the different source classes.

The upper limits derived in this paper constraint several prevailing neutrino flux models. This underlines the necessity of calculation on the basis of new developments within astroparticle physics and numerical approaches. A unified model concerning acceleration processes in AGN would give the opportunity to examine a potential neutrino signal with respect to different AGN classes within the same framework. The numerical results could be applied to individual sources and to diffuse flux measurements. The interaction between the observation of resolved sources and diffuse photon and proton components of CRs is of high significance with respect as it could be shown in this paper.

Acknowledgements

We would like to thank Francis Halzen, Tanja Kneiske, Anita Reimer, Reinhard Schlickeiser, Karl Mannheim, Marek Kowalski, Elisa Resconi, Ty de Young, Soeb Razzaque and Werner Collmar for inspiring discussions and helpful comments on this work. Many thanks also to the entire ICECUBE Collaboration for useful comments and suggestions.

Support for PLB is coming from the AUGER membership and theory grant 05CU 5PD 1/2 via DESY/BMBF. JKB and WR acknowledge the support by the BMBF, grant 05 CI5PE1/0 and by the DFG, grant RH 35/2-3.

References

Achterberg, A. et al. (IceCube Coll.), 2007, astro-ph/0705.1315, submitted to Phys. Rev. D.

Achterberg, A., et al. (IceCube Coll.), 2007. Phys. Rev. D 75, 102001.

Achterberg, A., et al. (IceCube Coll. and P. L. Biermann), 2006. Astrop. Phys. 26, 282.

Aharonian, F., et al. (H.E.S.S. Coll.), 2006. Nature 440, 1018.

Alvarez-Muñiz, J., Mészáros, P., Dec. 2004. Phys. Rev. D 70 (12), 123001.

Bade, N., et al., 1998. Astron. & Astrophys. 334, 459.

Becker, J. K., Biermann, P. L., Rhode, W., 2005. Astropart. Physics 23, 355.

Beckmann, V. et al., 2003. Astro. & Astrophys. 401, 927.

Beckmann, V., et al., 2006. Astrophys. J. 638, 642.

Biermann, P. L., Kusenko, A., 2006. Physical Review Letters 96 (9), 091301.

Biermann, P. L., Strom, R. G., Falcke, H., 1995. Astron. & Astrophys. 302, 429.

Bouwens, R. J., Illingworth, G. D., 2006. Nature 443, 189.

Brandt, W. N., Hasinger, G., 2005. Ann. Rev. Astron. Astrophys. 43, 827.

Chiang, J., Mukherjee, R., 1998. Astrophys. J. 496, 752.

Donea, A. C., Biermann, P. L., 1996. Astron. & Astrophys. 316, 43.

Dunlop, J. S., Peacock, J. A., 1990. Month. Not. Roy. Astr. Soc. 247, 19.

Falcke, H., Biermann, P. L., 1995. Astron. & Astrophys. 293, 665.

Falcke, H., Biermann, P. L., 1999. Astron. & Astrophys. 342, 49.

Falcke, H., Malkan, M. A., Biermann, P. L., 1995. Astron. & Astrophys. 298, 375.

Faranoff, B. L., Riley, J. M., 1974. Month. Not. Roy. Astr. Soc. 167, 31P.

Gehrels, N., Michelson, P., 1999. Astropart. Physics 11.

Gopal-Krishna, Biermann, P. L., Wiita, P. J., 2004. Astrophys. J. Let. 603, L9.

Hodges, J., et al., August 2006. In: TeV Particle Astrophysics II. <http://icecube.wisc.edu/tev/presentations.php>.

Iye, M., et al., 2006. Nature 443, 186.

Kanbach, G., et al., 2004. The MEGA project. New Astron. Review 48, 275.

Kappadath, S. C., et al., 1996. Astron. & Astrophys. Supp. 120, C619.

Kneiske, T. M., et al., 2004. Astron. & Astrophys. 413, 807.

Laurent-Muehleisen, S. A., et al., 1999. Astrophys. J. 525, 127.

Loeb, A., Waxman, E., 2006. Journ. of Cosm. and Astr. Phys. 5, 3.

Longair, M. S., 1998. Galaxy Formation. Springer.

Mahadevan, R., 1998. Nature 394, 651.

Mannheim, K., 1995. Astropart. Physics 3, 295.

Mannheim, K., Protheroe, R. J., Rachen, J. P., 2001. Phys. Rev. D 63, 23003.

Mannheim, K., Schulte, M., Rachen, J., 1995. Astron. & Astrophys. 303, L41.

Mannheim, K., et al., 1996. Astron. & Astrophys. 315, 77.

Mücke, A., et al., 2003. Astroparticle Physics 18, 593.

Münich, K., et al., August 2005. In: 29th International Cosmic Ray Conference.

ence. astro-ph/0509330.

Nellen, L., Mannheim, K., Biermann, P. L., 1993. Phys. Rev. D 47, 5270.

O'Dea, C. P., Baum, S. A., 1997. Astron. J. 113, 148.

Olbers, H. W. M., 1826. Über die Durchsichtigkeit des Weltraums. Astron. Jahrb. für das Jahr 1826. Later published in the collection *Olbers. Sein Leben und seine Werke*, editor: C. Schilling, publisher: Julius Springer, year: 1894.

Rachen, J., Mannheim, K., Biermann, P. L., 1995. Astron. & Astrophys. 310, 371.

Rybicki, G. B., Lightman, A. P., 1979. Radiative processes in astrophysics. J. Wiley & Sons, Inc.

Sanders, D. B., et al., 1989. Astrophys. J. 347, 29.

Schmidt, M., 1972. Astrophys. J. 176, 303.

Sinnis, G., Smith, A., McEnery, J. E., 2005. In: Novello, M., Perez Bergliaffa, S., Ruffini, R. (Eds.), The Tenth Marcel Grossmann Meeting. On recent developments in theoretical and experimental general relativity, gravitation and relativistic field theories. p. 1068.

Smith, A., et al., August 2006. The next generation all-sky gamma-ray telescope: mini-HAWC. In: TeV Particle Astrophysics II. <http://icecube.wisc.edu/tev/presentations.php>.

Sreekumar, P., et al., 1998. Astrophys. J. 494, 523.

Stecker, F. W., 2005. Phys. Rev. D 72 (10), 107301.

Stecker, F. W., 2007. Astroparticle Physics 26, 398.

F. W. Stecker, O. C. de Jager, and M. H. Salamon. *Astroph. Journal Let.*, 390:L49, 1992.

Stecker, F. W. and Salamon, M. H., 1996. Space Science Reviews 75, 341.

F. W. Stecker and M. H. Salamon. In S. Ritz, N. Gehrels, and C. R. Shrader, editors, *AIP Conf. Proc. 587: Gamma 2001: Gamma-Ray Astrophysics*, page 432, 2001.

Strong, A. W., Moskalenko, I. V., Reimer, O., 2005. In: AIP Conf. Proc. 745: High Energy Gamma-Ray Astronomy. p. 585.

Teshima, M., August 2006. TeV Particle Astrophysics II, Madison, . Presentation at www.icecube.wisc.edu/tev/.

Waxman, E., Bahcall, J., 1999. Phys. Rev. D 59, 23002.

Willott, C. J., et al., 2001. Month. Not. Roy. Astr. Soc. 322, 536.